NASA
Technical
Paper
2618

September 1986

Development and Flight Test of an Experimental Maneuver Autopilot for a Highly Maneuverable Aircraft

Eugene L. Duke,
Frank P. Jones,
and Ralph B. Roncoli

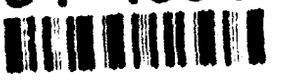

NASA Technical Paper 2618

1986

Development and Flight Test of an Experimental Maneuver Autopilot for a Highly Maneuverable Aircraft

Eugene L. Duke,
Frank P. Jones,
and Ralph B. Roncoli

Ames Research Center
Dryden Flight Research Facility
Edwards, California

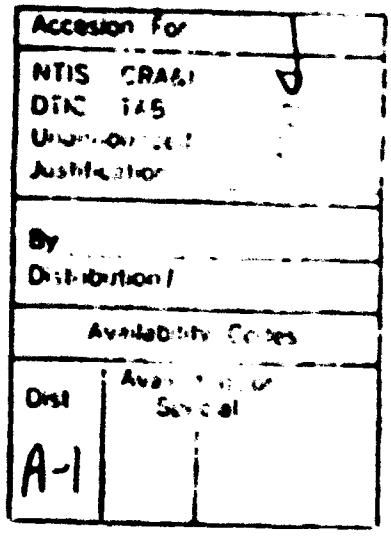

National Aeronautics and Space Administration

Scientific and Technical Information Branch

SUMMARY

This report presents the development of an experimental flight test maneuver autopilot (FTMAP) for a highly maneuverable aircraft. The essence of this technique is the application of an autopilot to provide precise control during required flight test maneuvers. This newly developed flight test technique is being applied at the Dryden Flight Research Facility of NASA Ames Research Center. The FTMAP is designed to increase the quantity and quality of data obtained in flight test. The technique was developed and demonstrated on the highly maneuverable aircraft technology (HiMAT) vehicle. This report describes the HiMAT vehicle systems, maneuver requirements, FTMAP development process, and flight results.

INTRODUCTION

To meet the research needs of the highly maneuverable aircraft technology (HiMAT) project, a new flight test technique was developed at the Dryden Flight Research Facility of NASA Ames Research Center (Ames-Dryden). The essence of this flight test technique is the application of an autopilot to provide precise control during required flight test maneuvers, such as pushover pullups, windup turns, and "rocking-horse" maneuvers. This technique, the flight test manuever autopilot (FTMAP), was applied to the HiMAT vehicle because of the problems in flying the vehicle at high angles of attack and elevated load factors. The problems were such that the pilot received no motion or usual visual cues, and the aircraft experienced wing rock and buffet at the high angles of attack at which data were to be collected.

The FTMAP is the extension of previous flight test trajectory guidance research at Ames-Dryden (ref. 1) and represents the first closed-loop application of this pilot-aiding technique. The FTMAP was designed to provide precise, repeatable control of the HiMAT vehicle during certain prescribed maneuvers so that a large quantity of high-quality test data could be obtained in a minimum of flight time.

The FTMAP has been used for various maneuvers, including straight-and-level flight, level accelerations and decelerations, pushover pullups, excess-thrust windup turns, thrust-limited windup turns, and the rocking-horse maneuver.

This report discusses the development of the FTMAP within the context of the HiMAT systems and flight test maneuver requirements. The details of the HiMAT system implementation determined the mechanization technique used with the FTMAP; the specific maneuver requirements of the HiMAT research program determined the trajectories selected for automation. The development of the FTMAP is detailed from linear analysis through nonlinear simulation to application in flight. The analytic models and development tools used in this process are described in their context of application. Flight test results are included to illustrate the FTMAP operational effectiveness.

While developed specifically for the HiMAT remotely piloted research vehicle (RPRV), the FTMAP represents a broadly applicable flight test technique that provides the pilot with a means of simultaneously controlling multiple parameters to meet demanding tolerances. This technique is extendable to either manned aircraft or aircraft having less performance capability and maneuverability than the HiMAT vehicle.

NOMENCLATURE

Where appropriate, parameters are referenced to fuselage body axes according to right-hand sign conventions.

A	state matrix
A/B	afterburner

ADC	analog-to-digital converter
a_n	normal acceleration, g
a_y	lateral acceleration, g
B	control matrix
BCS	backup control system
DAC	digital-to-analog converter
E_s	specific energy, m (ft)
FTMAP	flight test maneuver autopilot
f_k	primary control system feedback gain or function
G	observation matrix
G-ERR/ ILS-GLSP	switch to selec. between trajectory guidance or landing display
g	gravitational acceleration, m/sec^2 (ft/sec^2)
H	feedforward matrix
HiMAT	highly maneuverable aircraft technology
h	altitude, m (ft)
$\dot{h}$	altitude rate, m/sec (ft/sec)
I/O	input-output
K	feedback gain
K_{ab}	throttle forward-loop gain
K_M	lateral gain factor
K_{N_T}	pitch-axis forward-loop gain for primary control system
K_{OB}	onboard pitch-rate feedback gain, sec
K_{P_D}	lateral stick gain
$K_{\bar{q}}$	pitch-axis dynamic-pressure gain
$K_{q_{tc}}$	throttle impact-pressure error gain, $deg-m^2/kg-sec$ ($deg-ft^2/lb-sec$)
$K_{\dot{q}_{tc}}$	throttle impact-pressure rate gain, $deg-m^2/kg$ ($deg-ft^2/lb$)
K_θ	pitch-axis stick gain for primary control system, deg/cm-sec (deg/in-sec)
LED	light-emitting diode
M	Mach number
M_{ref}	zero-excess-thrust Mach number
P_s	specific power, m/sec (ft/sec)
PCS	primary control system
PLA	power lever angle (equivalent throttle), deg
p	roll rate, deg/sec
p_a	ambient pressure, kg/m^2 (lb/ft^2)
$\dot{p}_a$	ambient (static) pressure rate, kg/m^2-sec (lb/ft^2-sec)

q	pitch rate, deg/sec
$\bar{q}$	dynamic pressure, kg/m^2 (lb/ft^2)
q_c	impact pressure, kg/m^2 (lb/ft^2)
$\dot{q}_c$	impact-pressure rate, kg/m^2-sec (lb/ft^2-sec)
RPRV	remotely piloted research vehicle
r	yaw rate, deg/sec
s	Laplace variable
t	time, sec
u	x-axis velocity component, m/sec (ft/sec)
V	total vehicle velocity, m/sec (ft/sec)
$\dot{V}$	total vehicle acceleration, m/sec (ft/sec)
v	y-axis velocity component, m/sec (ft/sec)
w	z-axis velocity component, m/sec (ft/sec)
z	z-transform variable
α	angle of attack, deg
$\dot{\alpha}$	angle-of-attack rate, deg/sec
α_o	trim or nominal angle of attack, deg
Δa_n	difference between measured normal acceleration and reference normal acceleration, g
Δh	altitude error from commanded altitude, m (ft)
ΔM	Mach error from commanded Mach number
Δt_α	time that angle-of-attack command is to be held during pushover pullup, sec
δa_p	lateral stick position or equivalent lateral stick position, cm (in)
δe	elevator position, deg
δe_p	longitudinal stick position or equivalent longitudinal stick position, cm (in)
δL	total longitudinal surface deflection, deg
δr	rudder position, deg
δv_a	asymmetric elevon deflection, deg
δv_s	symmetric elevon deflection, deg
θ	pitch angle, deg
ϕ	bank angle, deg

Subscripts:

a	ambient or asymmetric
ab	afterburner
cmd	command value
D	direct control path gain
I	integral control path gain
k	scheduled gain function

max	maximum or limit value
min	minimum or limit value
N	normal control law path (as opposed to boundary limiter path)
n	normal
o	trim value
ref	reference value
T	thrust
y	lateral

Vectors:

$\underline{u}$	control vector
$\underline{x}$	state vector
$\dot{\underline{x}}$	derivative of the state vector with respect to time
$\underline{y}$	observation vector
$[\ldots]^T$	column vector notation

HiMAT SYSTEMS DESCRIPTION

The HiMAT vehicle (fig. 1) was designed to incorporate technological advances in many fields: close-coupled canard configuration, aeroelastic tailoring, advanced transonic aerodynamics, advanced composite and metallic structures, digital fly by-wire controls, and digitally implemented integrated propulsion control systems (ref. 2). The HiMAT RPRV (fig. 2) is a 0.44-scale version of an envisioned full-scale fighter aircraft with an 8-g sustained-turn maneuver capability at Mach 0.90 and an altitude of 7600 m (25,000 ft).

The operational concept (fig. 3) for the HiMAT vehicle is similar to that for previous RPRVs flown at Ames-Dryden. The 1530-kg (3370-lb) vehicle is air-launched from a B-52 aircraft at 13,700 m (45,000 ft) and carries 300 kg (660 lb) of fuel for the J85-21 engine. The vehicle is flown under the control of a NASA research test pilot located in a ground-based RPRV facility cockpit. Flight test activity is monitored on the ground by use of telemetry downlink. Flight control laws for both primary and backup operation are implemented through two ground-based and two airborne digital computers. The vehicle is equipped with landing skids and forward-looking television for horizontal recovery on the surface of an Edwards dry lakebed.

In the primary mode of operation (fig. 4), aircraft sensor data are transmitted to the ground by a telemetry downlink. The downlinked data are used to drive the ground cockpit displays; the data are also used as input to the ground-based primary control system (PCS) computer The control law computer combines the pilot input commands with the downlinked aircraft sensor data in the execution of the HiMAT control laws. The computer then formats a servo-actuator command for each of the vehicle control surfaces and throttle. These surface commands are output to the uplink encoder and then transmitted to the aircraft (ref. 3).

MANEUVER REQUIREMENTS

To accomplish the primary project research objectives, several maneuvers were required, including level accelerations and decelerations, pushover pullups, excess-thrust windup turns, thrust-limited windup turns, level turns, and the rocking-horse maneuver. These maneuvers were to be performed with a precision that necessitated the development of a technique to provide automatic multiple-axis control. Not only were terminal conditions specified to exacting accuracies, but the rates at which these conditions were to be achieved were an additional constraint. For a pilot using manual control and

normal piloting techniques, the rate of onset of a flight maneuver is the most demanding requirement. The maneuvers used angle-of-attack command or normal-acceleration command variables. The design goal was to control the rate of onset by linearly increasing the command variable at 0.25 deg/sec for angle-of-attack commanded maneuvers and 0.2 g/sec for normal-acceleration commanded maneuvers. This was to be accomplished while controlling the vehicle to tolerances of ±0.5° angle of attack or ±0.5-g normal acceleration, ±0.01 Mach, and ±150-m (±500-ft) altitude for the collection of aerodynamic, structural, flutter, and overall performance data. A description of each maneuver, its use, and the specific performance requirements for that maneuver are described in the following sections.

Level Accelerations and Decelerations

A level acceleration or deceleration is a 1-g, wings-level maneuver performed at constant altitude with increasing or decreasing Mach number. During a level acceleration or deceleration, longitudinal stick is used to control altitude, lateral stick is used to control roll attitude, and throttle is used to control Mach number. These maneuvers are used for airspeed calibrations, to determine climb performance, and to obtain overall performance data. These maneuvers are required to be performed at a constant altitude within ±150 m (±500 ft); the target Mach number is to be achieved without overshoot.

Pushover Pullups

A pushover pullup is a wings-level maneuver that can be performed at either a constant throttle setting or a constant Mach number. The maneuver consists of varying the aircraft angle of attack α about the trim condition α_0. Figure 5 illustrates the pitch-axis task for the pushover-pullup maneuver. The stick is pushed forward until the measured angle of attack reaches a specified angle-of-attack increment $\Delta\alpha$ below the trim conditions. This angle of attack is held for a predetermined condition-hold time Δt_α. Then the stick is pulled back past the trim point and held until the measured angle of attack increases to the specified $\Delta\alpha$ above the trim angle of attack. After the hold time, the stick is moved forward until the aircraft returns to straight-and-level flight. The commanded rate of change of angle of attack $\dot{\alpha}_{cmd}$ determines the slope of the angle-of-attack time history. During this maneuver, lateral stick is used to maintain a wings-level condition.

For the fixed-throttle pushover-pullup maneuver, Mach number is not controlled and the throttle remains constant throughout the maneuver. Similar to level accelerations and decelerations, the fixed-throttle maneuver is a two-axis task, which requires longitudinal and lateral control. However, the constant-Mach maneuver is a three-axis task that also requires active control of Mach number with the throttle. During the pushover-pullup maneuver in which a constant Mach number is maintained, the longitudinal and airspeed axes are strongly coupled.

The pushover-pullup maneuver is used to obtain drag data and wing and canard pressure data at angles of attack above and below trim. The maneuver is to be performed to a measured angle of attack within ±0.5° of the commanded angle-of-attack profile. In addition, the rate of change of angle of attack must be maintained at 0.50 deg/sec during the maneuver. The time Δt_α for which the end condition ($\alpha \pm \alpha_{cmd}$) is to be held was originally specified as 5 sec, but was later changed to zero. For the constant-Mach pushover

pullup, the tolerance in Mach error is ±0.01 Mach.

Turns

An excess-thrust windup turn, a thrust-limited windup turn, and a level turn are all elevated normal-acceleration maneuvers. Longitudinal stick is used to control angle of attack or normal acceleration, the lateral stick is used to control altitude rate, and the throttle is used to control Mach number. The excess-thrust windup turn is a turn in which normal acceleration, load factor, and angle of attack are increased to a target value at a constant altitude and constant Mach number. The thrust-limited windup turn is performed not at constant altitude, but with the nose of the aircraft pointing slightly downward. This aligns the gravity vector more closely with the aircraft body axis to act as a thrust-aiding force, so that altitude is traded for Mach number. The level turn is a constant normal-acceleration version of the excess-thrust turn.

These turns are used to provide flight conditions to measure wing loads, wing deflection, wing pressures, drag, and buffet, as well as to gather stability and control data at elevated normal acceleration and angle of attack. For the HiMAT program, each of the three turns is required to be angle-of-attack commanded or normal-acceleration commanded, with the target condition specified in terms of an angle of attack or a normal acceleration, respectively. During these turns, the objective is to maintain altitude within ±150 m (±500 ft) and to maintain Mach number within ±0.01 of the nominal. The commanded parameter from the trim to the target condition is to be increased at a specified rate of 0.25 deg/sec for angle-of-attack commanded turns and 0.2 g/sec for normal-acceleration commanded turns. An additional constraint is that the target condition be achieved to a tolerance of ±0.5° angle of attack or ±0.5-g normal acceleration.

The command rate is the most demanding requirement for the pilot because, as the normal acceleration of a maneuver increases, so does the difficulty of controlling the vehicle to maintain the other mission tolerances. To illustrate the complexity of the piloting task as a function of increasing normal acceleration, figure 6 shows the bank-angle requirements for a range of normal accelerations. Figure 6 is based on the normal-acceleration tolerance (±0.5 g) and the relationship for a constant-altitude turn,

$$\phi = \cos^{-1} \frac{1}{a_n}$$

where ϕ is the bank angle and a_n is the normal acceleration. The graph in figure 6 shows that the acceptable range for bank angle decreases dramatically as the target normal acceleration increases. Thus, lateral control of the vehicle becomes more demanding as the target normal acceleration increases. Because the orientation of the lift vector determines the altitude rate of the vehicle, the main effect of bank-angle variations is altitude error. The altitude rate generated by a bank-angle error increases as the normal acceleration increases.

While figure 6 illustrates the decreasing bank-angle tolerance as a function of target normal acceleration, this same plot could be used to show the relationship of time until the altitude tolerance is exceeded as a function of normal acceleration. Thus, not only does the tolerance for bank-angle error decrease as a function of increasing target normal acceleration, but the amount of time until altitude is out of tolerance decreases, thereby requiring more attention to the lateral axis. The windup turn is a highly coupled three-axis task requiring longitudinal,

ateral, and airspeed control. Not nly does a change in angle of attack nd normal acceleration require a com- ensating change in bank angle to main- ain the specified altitude, but an mmediate throttle change is required o maintain Mach number to compensate or changing drag.

Rocking-Horse Maneuvers

A rocking-horse maneuver is per- formed after a windup turn has stabi- ized to the zero-excess-thrust con- ition. The purpose of the manuever s to gather performance data at Mach umbers and load factors near the appar- nt zero-excess-thrust condition to fix the exact zero-excess-thrust condition. This condition is important because it letermines the maximum sustained turning capability of the vehicle in a given flight condition. Because zero excess thrust occurs when the available thrust is equal to the drag, any increase in normal acceleration must be accompanied by either an altitude or a velocity loss. The rocking-horse manuever is a highly coupled two-axis task requiring longitu- dinal and lateral control, which creates even more pilot workload than the wind- up turn. Because the throttle is fixed at maximum afterburner, the maneuver requires only stick action, albeit highly coordinated.

Figure 7 illustrates the normal acceleration and Mach number charac- teristics of a single cycle of the rocking horse. Once the vehicle is at the zero-excess-thrust condition and the thrust has stabilized at maximum afterburner, the longitudinal stick is moved rapidly aft until some specified increase in normal acceleration Δa_n has been obtained. This aft longitudinal stick movement must be accompanied by lateral stick activity to increase bank angle and maintain level flight. The elevated load factor condition is main- tained until Mach number has decreased a specified amount ΔM from the zero- excess-thrust Mach number M_{ref}. When the desired Mach number ($M_{ref} - \Delta M$) has been reached, the longitudinal stick is moved forward quickly to achieve $-\Delta a_n$. This longitudinal stick movement is accompanied by lateral stick action to decrease the bank angle and maintain level flight. The forward stick posi- tion is held until Mach number has increased to $M_{ref} + \Delta M$; the stick is then moved aft until normal acceleration at zero excess thrust a_{n_o} is achieved.

Because the rocking-horse maneuver is flown at maximum afterburner, fuel consumption is high and the amount of time available for maneuvering is lim- ited. The only constraint on the ini- tial windup turn is that it end at a specific altitude and Mach number when excess thrust decreases to zero. However, if the windup turn to the zero-excess-thrust condition can be controlled, useful wing loads, pres- sure, and deflection data can also be collected during the turn. As excess thrust is reduced to zero, the ability to change total vehicle energy also decreases to zero. The vehicle specific energy E_s is given by the relationship

$$E_s = h + \frac{V^2}{2g}$$

where h is altitude, V is total veloc- ity, and g is the acceleration due to gravity. The derivative of this quan- tity with respect to time yields spe- cific power P_s where

$$P_s = \frac{d}{dt} E_s = \dot{h} + \frac{\dot{V}V}{g}$$

which is used as the specification parameter for the zero-excess-thrust condition of P_s equal to 0 ± 8 m/sec (0 ± 25 ft/sec). The rate of change of normal acceleration is specified as 5 g/sec. The Δa_n has a tolerance of ±0.5 g, and ΔM is specified as the point at which stick reversal occurs.

FTMAP DESCRIPTION

To provide the capability to perform the required research maneuvers, the FTMAP operates as an outer loop to the FCS, replacing the pilot in the closed-loop flight system (fig. 8). When the FTMAP is engaged, the normal pilot input commands are replaced by corresponding commands generated by the FTMAP. These FTMAP-generated commands are the result of feedback control laws that operate on error signals derived by comparing measured vehicle parameters with a dynamically computed trajectory. This computed trajectory corresponds to the flight test maneuver selected by the pilot.

Appendix A presents a detailed description of the FTMAP systems and a discussion of both operational characteristics and operational mechanization of the FTMAP. Appendix B provides a description of the FTMAP control laws, appendix C details the development of the FTMAP from linear analysis through simulation and flight, and appendix D describes special HiMAT instrumentation used with the FTMAP.

FLIGHT RESULTS

Three HiMAT flights were used for FTMAP development (ref. 4). On the first two flights, the FTMAP was used only for altitude hold during cruise, accelerations, and decelerations at constant altitude. Based on this flight experience, a longitudinal dynamic-pressure gain schedule was added to the FTMAP control laws. On the third flight, the FTMAP was used for three range-positioning, low-q turns at an altitude of 12,000 m (40,000 ft). These three windup turns were performed at Mach 0.90, 0.95, and 1.10. The success of the FTMAP on these flights encouraged its use on subsequent flights.

On the fourth flight, the FTMAP was used to collect flight research data. The FTMAP successfully controlled the HiMAT through a constant-altitude cruise, a constant-altitude deceleration, a windup turn at low dynamic pressure, and a constant-Mach push-over pullup. However, when the windup turn to the design condition of 8 g at Mach 0.90 and 7600-m (25,000-ft) altitude was initiated, a lateral instability was experienced. This problem (discussed in app. C) was corrected before the next HiMAT flight one week later. On that flight, the FTMAP successfully controlled the HiMAT vehicle for all data collection maneuvers. The use of the FTMAP in flight accounted for 53 percent of the 25.5-min total flight time from launch to touchdown.

For the remaining HiMAT flights, the FTMAP was used for almost all data collection maneuvers. On the seventh flight, the thrust-limited windup turn was demonstrated under FTMAP control. The FTMAP was used during the remaining flights with only minor modifications.

Because of the success of the FTMAP development and flight application, only a limited number of research maneuvers were flown manually by the pilots after the FTMAP became operational. The results of this limited sample of maneuvers are used, where applicable, to compare FTMAP-flown and manually flown maneuvers. A description of the FTMAP-flown maneuvers is presented in the following sections.

Altitude Hold

Although not required in the FTMAP design specification, the altitude-hold maneuver was used to establish constant-Mach and constant-altitude cruise, as well as to control altitude during decelerations and accelerations. Figure 9 shows a wings-level, constant-altitude, constant-Mach cruise at a nominal Mach 0.80 and a 12,200-m (40,000-ft) altitude. The FTMAP controls the vehicle at the engagement altitude and commanded Mach

number to within the resolution of the data system.

The constant-altitude deceleration shown in figure 10 was flown at a nominal altitude of 7600 m (25,000 ft) and a Mach range from approximately 0.70 to 0.50. Once again, the excellent FTMAP control and stability are evident. A level acceleration from approximately Mach 0.50 to 0.80 is shown in figure 11. The key feature of these maneuvers is the control of altitude to within the resolution of the data system. For the accelerations and decelerations, the lack of overshoot in Mach number at the final condition illustrates the desired well-damped performance.

As can be seen from figures 9 to 11, the FTMAP provided a means of collecting data at constant altitude to exacting tolerances. This system provided high-quality, consistent cruise and performance data. Particularly noteworthy is the demonstration of the Mach number control feature. The level accelerations and decelerations were performed smoothly and at constant Mach rates. The target Mach number was achieved without overshoot.

Pushover-Pullup Maneuvers

The constant-Mach pushover pullup was demonstrated in flight as an example of the pushover-pullup class of maneuvers. This maneuver was performed to the specified requirements with only minor deviations beyond Mach number tolerance. Figure 12 compares three FTMAP pushover pullups at nominal conditions of a 6100-m (20,000-ft) altitude and Mach 0.80. As shown in figure 12, the data obtained from these maneuvers are repeatable from flight to flight. The quality of the data is evident from the time histories of the maneuvers in figures 12 to 15. These figures demonstrate that the FTMAP performed the pushover-pullup maneuvers throughout the HiMAT flight envelope.

As demonstrated by the altitude-rate time histories, these maneuvers are highly dynamic. However, Mach number is maintained close to the nominal condition. The angle-of-attack time histories show the smooth control of the FTMAP from pushover-pullup initiation to exit phase initiation. During the exit phase of the maneuver, the FTMAP transitions from the angle-of-attack control mode to the altitude-hold control mode. The altitude recovery portion of this maneuver is actually performed using the altitude-hold control capability of the FTMAP with the nominal altitude as reference.

Windup Turns

Figure 16 compares two manually flown windup turns. These maneuvers are initiated from a wings-level, 1-g condition at a nominal altitude of 7600 m (25,000 ft) and Mach 0.90. The objective of each maneuver is to increase either the normal acceleration at a rate of 0.2 g/sec or the angle of attack at a rate of 0.25 deg/sec until the design condition is achieved. Mach number is to be held to ±0.01 Mach, and altitude is to be within ±150 m (±500 ft) of the nominal. Two features of these maneuvers are important — maneuver quality and maneuver consistency. The difficulty of flying these maneuvers is apparent from the time histories. In both maneuvers, the rates of increase of normal acceleration and angle of attack are irregular and erratic. Both the Mach number and altitude tolerances are exceeded. There is little repeatability from maneuver to maneuver.

In contrast, three FTMAP-flown windup turns shown in figure 17 are virtually identical. The rates of increase for both angle of attack and normal acceleration are regular and controlled. Altitude tolerance is maintained throughout the maneuver. However, the Mach number tolerance is still exceeded. This maneuver qual-

ity, repeatability, and hence, predictability were demonstrated throughout the HiMAT flight envelope. Another key point of this comparison is the difference in elapsed time for maneuver execution. The pilot-flown maneuvers require approximately 80 sec, whereas the FTMAP-flown maneuvers are completed within 50 sec.

Figure 18 illustrates both the supersonic performance of the FTMAP and its ability to achieve and maintain a flight condition. The maneuver is a normal-acceleration commanded windup turn to 2 g at an altitude of 12,200 m (40,000 ft) and Mach 1.10. Once the 2-g turn is achieved, the FTMAP recovers Mach number to within the resolution of the data system. The flight condition is held almost without deviation for approximately 40 sec. Figure 19 shows time histories from an angle-of-attack commanded windup turn to 12° angle of attack. The maneuver was performed at Mach 0.80 and an altitude of 9800 m (32,000 ft). This maneuver again illustrates the capability of the FTMAP to control the HiMAT vehicle in a precise, predictable way. The rates of onset of both angle of attack and normal acceleration are regular and consistent. Both Mach number and altitude are held to the specified tolerances.

These two windup turn maneuvers (figs. 18 and 19) are representative of the class of maneuvers in which the FTMAP excelled and in which all design specifications were met. The common feature is the absence of the transition from core engine to afterburner. The supersonic maneuver (fig. 18) was performed entirely in afterburner. The subsonic maneuver (fig. 19) was performed without the use of afterburner. On the other hand, the FTMAP maneuvers shown in figure 17 began without afterburner and transitioned into afterburner as angle of attack increased. This transition occurred during the period when the slopes of the angle-of-attack and normal-acceleration time histories leveled out. The logic used to detect and compensate for this transition is described in appendix C.

Figure 20 is a time history showing elevator doublets performed for parameter identification purposes during an FTMAP-controlled level turn. The maneuver was performed at Mach 0.80 and an altitude of 4600 m (15,000 ft) at a 6-g normal acceleration. This time history illustrates the ability of the FTMAP to accommodate disturbances. The ability to collect repeatable data is evident. The response of the system is virtually identical for each elevator doublet. The flight condition is maintained to well beyond the design specifications of the FTMAP.

The two thrust-limited windup turns shown in figures 21 and 22 illustrate the performance of the FTMAP logic in detecting the zero-specific-power ($P_S = 0$) condition and controlling the HiMAT vehicle during a descending spiral by trading altitude for Mach number. In the turn at Mach 0.90 and an altitude of 7600 m (25,000 ft), the logic to detect the thrust-limited condition allows the vehicle to gain an additional 1° angle of attack and 2-g normal acceleration while bringing the Mach number back to within a tolerance of ± 0.01 Mach for part of the maneuver (fig. 21). For the supersonic maneuver at Mach 1.20 and an altitude of 12,200 m (40,000 ft), the thrust-limited maneuver resulted in data for approximately 2° more angle of attack and 3 g more normal acceleration than would have been available without this logic (fig. 22). However, as shown in the Mach-number time history, this logic caused the vehicle to accelerate excessively and to exceed tolerance.

The performance of the thrust-limited control was demonstrated in flight. The ability to detect and compensate for the thrust-limited condition was judged to be tolerable but did not meet the Mach tolerance specification. As thrust-limited control performance

was acceptable, further development was curtailed and this control logic was not refined.

FUTURE RESEARCH

The application of the FTMAP on the HiMAT vehicle represents a proof of concept rather than a finished production-type system. While the FTMAP performed exceptionally well, not all design goals met the required tolerances. Additionally, many lessons were learned concerning requirements for an FTMAP system. This section of the report attempts to define the key areas in which further maneuver autopilot research is needed.

The most significant problem encountered during the development and flight demonstration of the FTMAP was the sensitivity of the autopilot to the aerodynamic model. This is not a problem unique to control law design for an FTMAP, but the consequences are more severe than for conventional control law design. If the FTMAP is to be a tool for the initial flight test of a new vehicle, the design must be more robust and probably more adaptive. To restrict the FTMAP to vehicles with well-known and well-modeled aerodynamics is to limit its application so severely that the FTMAP would have little practical value as a generic flight test technique.

Most of the problems encountered during FTMAP flight test were related to Mach number control. These problems occurred during the transition from core engine to afterburner and after the thrust-limited condition. Both of these regions are highly nonlinear transitions that are somewhat vehicle dependent. However, techniques can be developed to regulate the rate of onset of angle of attack as military power is approached. The control of a vehicle in a thrust-limited turn is a difficult but achievable task. These two aspects of Mach number control should be explored on future projects.

The development and demonstration of additional maneuvers are areas of future FTMAP research. These include not only the demonstration of maneuvers already developed, but also the development and demonstration of totally new maneuvers based on the capabilities of the FTMAP. Two performance maneuvers were developed for the FTMAP but were not demonstrated in flight: the constant-throttle pushover-pullup and the rocking-horse maneuvers. These maneuvers would be a useful adjunct to the related flight research maneuvers for the FTMAP.

In particular, the rocking-horse maneuver is an extremely demanding and difficult maneuver. Figure 23 illustrates two pilot-flown rocking-horse maneuvers. The supersonic maneuver shown in figure 23(a) was performed at nominal conditions of Mach 1.40 and an altitude of 12,200 m (40,000 ft). The subsonic maneuver shown in figure 23(b) was flown about nominal conditions of Mach 0.90 and an altitude of 7600 m (25,000 ft). A feature most apparent from these two time histories is the altitude range. The rocking-horse maneuver is supposed to be a constant-altitude maneuver. The difficulty of controlling altitude is shown in the altitude-rate time histories. The pilot must constantly compensate for altitude rate that is generated as a consequence of changing the normal acceleration of the vehicle. Because the information needed to fly this maneuver (altitude, Mach number, and normal acceleration) is on three separate instruments, the task is even more difficult for the pilot.

Two rocking-horse maneuvers flown by the FTMAP in the HiMAT simulator are shown in figure 24. The maneuver shown in figure 24(a) was executed at simulated conditions of Mach 1.10 and an altitude of 12,200 m (40,000 ft). The

maneuver shown in figure 24(b) was executed at simulated conditions of Mach 1.20 and an altitude of 7600 m (25,000 ft). Because these maneuvers were executed on the simulator and not in flight, they should not be compared too closely with the pilot-flown rocking-horse maneuvers. However, the features to be noted in the simulated FTMAP maneuvers are the altitude control, the virtual absence of altitude rate during the rocking-horse maneuver itself, and the repeatability of each cycle of the maneuver. Based on the experience with the FTMAP in a level turn (fig. 20), the flight results would probably be about the same as the simulator results presented here.

Flight research maneuvers that could be performed by an FTMAP include (1) altitude and Mach number profiles flown at constant Reynolds number or dynamic pressure with a specified angle of attack, and (2) constant-altitude accelerations and decelerations performed at a specified angle of attack or normal acceleration. These maneuvers are even more demanding of the pilot than the rocking-horse maneuver and would benefit greatly from automation.

A limitation imposed on the FTMAP by the pilot interface with the system was the need to achieve altitude by manually flying the vehicle to the desired altitude. In fact, the use of thumbwheel switches to select maneuvers and maneuver conditions was somewhat limiting. The pilot-FTMAP interface is one of the areas in which research would be beneficial. This will be a particularly important issue when the FTMAP is applied to a manned vehicle.

CONCLUDING REMARKS

An experimental flight test maneuver autopilot (FTMAP) was developed for the highly maneuverable aircraft technology (HiMAT) vehicle. This application of the FTMAP represents a proof of concept of an advanced flight test technique rather than a finished production-type system. The FTMAP was used to fly level accelerations and decelerations, constant-Mach pushover pullups, excess-thrust windup turns, and thrust-limited windup turns. All maneuvers for which it was designed, except the constant-throttle pushover-pullup and the rocking-horse maneuvers, were demonstrated in flight. The FTMAP performed exceptionally well — meeting and often exceeding the extremely demanding maneuver tolerances: Mach within ± 0.01, altitude within ± 150 m (± 500 ft), angle of attack within $\pm 0.5°$, and normal acceleration within ± 0.5 g. In some cases, the Mach number tolerance was not met. However, even in these instances, the FTMAP proved capable of controlling the HiMAT vehicle to tolerances comparable to those for a pilot using normal piloting techniques. This new technique has been demonstrated in flight and has proved to be a valuable tool.

The stated goals of the FTMAP development were to increase the quantity and quality of the data obtained in flight test. The objectives were to provide precise, repeatable control of the HiMAT vehicle during certain prescribed maneuvers and to ensure that a large quantity of high-quality test data could be obtained in a minimum of flight time. All these goals and objectives were met. The FTMAP increased the overall quality of maneuvers significantly beyond what could be obtained by manual control. The quantity of data was increased because the FTMAP performed maneuvers in less time than the pilot and also because maneuvers did not have to be repeated because of poor maneuver execution.

This report documents the development of the FTMAP from the defining of design requirements to FTMAP flight test. The application of linear analysis, modeling techniques, flight hardware-in-the-loop simulation, and flight test is illustrated. The result of this FTMAP development is an auto-

pilot that provides precise, repeatable control of an aircraft during prescribed maneuvers and also allows the collection of a large quantity of high-quality data. Although first applied to a high-performance remotely piloted research vehicle (RPRV), the FTMAP represents a broadly applicable flight test technique that has the potential to benefit any flight program. The FTMAP provides the pilot with a powerful aid that allows multiple parameters to be controlled simultaneously to exacting tolerances.

National Aeronautics and Space Administration
Ames Research Center
Dryden Flight Research Facility
Edwards, California, August 23, 1984

APPENDIX A — DETAILED FTMAP SYSTEMS DESCRIPTION

The FTMAP was developed to satisfy the project requirements for precise, repeatable maneuvers. The operational characteristics and the operational mechanization of the FTMAP for the HiMAT system are described in this appendix. Figure 25 is an overview of the HiMAT-FTMAP simulation system showing the input panel and FTMAP control laws described in this section and the command generation function described in the simulation analysis section (app. C).

FTMAP Operational Characteristics

The FTMAP operates as an outer loop to the PCS shown in figure 4, employing two additional ground-based computers (fig. 26). In this system, while the FTMAP is engaged, the normal PCS pilot input commands (that is, longitudinal stick, lateral stick, and throttle position) are replaced by corresponding commands generated in the FTMAP computer. The pilot retains rudder pedal control to trim sideslip; no FTMAP input is required in the yaw axis. The PCS control laws execute in series with the FTMAP control laws and provide the inner-loop stability augmentation.

Both the FTMAP and the PCS computers receive inputs from downlink processing computers that provide subframe decommutation of the downlink data stream. The data available to the FTMAP computer are identical to those available to the PCS computer. The FTMAP computer accepts data from a cockpit input panel (figs. 25 and 27) that allows definition of the test condition parameters, such as maneuver number, angle of attack, normal acceleration, and Mach number. This input panel includes thumbwheel switches, an annunciator display, and two electromagnetic control switches for FTMAP engagement and manuever initiation (fig. 28).

The system configuration for incorporating the FTMAP into the basic HiMAT PCS was selected according to the availability of hardware and the convenience of mechanization. Because a duplicate set of control and decommutation computers was already available in the RPRV facility, these computers were used. If these computers had not been available, a simpler scheme, such as the inclusion of the FTMAP control laws within the PCS computer, could have been employed for the mechanization of the FTMAP.

The procedure for flying a maneuver with the FTMAP requires the pilot to fly to the desired test altitude. When altitude rate is within a nominal 15-m/sec (±350-ft/sec) window and the vehicle is at the target altitude, the FTMAP is engaged using the cockpit input panel. Each maneuver sequence consists of three phases: straight and level, maneuver control, and maneuver disengagement. Engagement of the FTMAP establishes a reference altitude and puts the FTMAP into a straight-and-level, altitude-hold mode. For the level acceleration and deceleration maneuvers, the straight-and-level phase of any of the manuevers could be used and selected independently of the other two phases, to provide an altitude-hold autopilot with Mach number control. During the maneuver control phase, the FTMAP flies the vehicle through the test maneuver and monitors the vehicle states to determine when the test conditions are met and whether any predefined mission limits are exceeded. This monitoring of predefined mission limits is used to determine whether the FTMAP should be allowed to continue a maneuver. If one of these limits is encountered, the FTMAP automatically enters the maneuver disengagement phase and returns the vehicle to straight-and-level flight at the reference altitude.

The FTMAP is equipped with six procedures for exiting a maneuver. In

three of these procedures, the FTMAP remains operative and performs a controlled exit; in the other three, it is completely disengaged. In its normal operation, the FTMAP performs a controlled exit from the maneuver phase, executing a smooth, gentle ramping out of bank angle and load factor and returning the aircraft to straight-and-level flight.

The exit phase, like the straight-and-level and maneuver phases, is indicated on the instrument panel. Immediately after an exit has been commanded, the exit indicator is illuminated and the maneuver indicator turns off. The exit phase does not ramp the aircraft completely back to straight and level. At a certain point, based on the bank angle of the aircraft, the FTMAP changes from the exit phase to the straight-and-level phase. The light-emitting diode (LED) annunciators on the instrument panel change accordingly. The FTMAP then attempts to regain the engagement altitude and the thumbwheel-selected Mach number.

The primary method of exiting a maneuver is to pull the maneuver switch to the off position. This immediately commands the exit phase, which begins to ramp the aircraft back to straight-and-level flight. The rate at which the aircraft returns to straight and level is dependent on the maneuver selected. In an angle-of-attack commanded windup turn, the aircraft ramps back to straight and level at an angle-of-attack rate of 1.60 deg/sec. In a normal-acceleration commanded windup turn, the ramping rate is 1.28 g/sec. The ramping rate during the exit phase of a pushover-pullup maneuver is 0.50 deg/sec, which is equivalent to the rate throughout the maneuver phase.

The normal manuever exit phase can also be triggered by reaching one of the preset limits incorporated into the FTMAP to reflect envelope limits imposed on the vehicle. These preset limits are based on the actual angle of attack, normal acceleration, dynamic pressure, and Mach number limits of the aircraft minus a tolerance value. The tolerance value provides a safety margin to prevent possible damage to the aircraft. This method ensures that an exit is commanded if a limit is reached, regardless of the maneuver selected. In a windup turn, the type of maneuver selected determines the ramping rate back to straight and level. For example, if the aircraft were in a normal-acceleration commanded windup turn and reach[illegible] an angle-of-attack limit, it woul[illegible] back to straight and level at [illegible] corresponding to a normal-acceleration commanded windup turn.

Another method of commanding a normal exit from a windup turn maneuver is based on a maneuver timer. When the FTMAP reaches its target condition, the maneuver timer starts. The FTMAP holds the target condition for the prescribed amount of time and then commands an exit. In both the envelope limits and maneuver timer methods described, the magnetic maneuver switch automatically returns to the off position when an exit is commanded by the FTMAP.

The three remaining procedures completely disengage the autopilot and return control to the pilot. The primary method of disengaging the autopilot is to squeeze the trigger switch on the control stick. Squeezing the trigger returns one or both of the FTMAP electromagnetic control switches to their original positions, depending on the current phase of FTMAP operation. The sound associated with the disengagement of the control switches provides the pilot with a positive aural indication that he has control of the aircraft.

An equally effective procedure to disengage the FTMAP is to put the magnetic level-cruise switch in the disengage position. If the aircraft is

in a maneuver, this action also causes the magnetic maneuver switch to move to the off position.

The third method of disengaging the autopilot involves the G-ERR/ILS-GLSP switch behind the thumbwheel switches (fig. 28). The G-ERR position provides the pilot with a special flight director display, while the ILS-GLSP position provides the pilot with instrument landing-glideslope guidance. When this switch is pushed forward to the ILS-GLSP position, the FTMAP disengages. Although not intended to be the primary means of disengagement, this method prevents the possibility of entering a manuever while attempting to land.

Totally disengaging the FTMAP causes the current stick and throttle positions to be sent to the PCS and hence to the vehicle. Thus, using one of these procedures that completely disengage the autopilot has the potential for introducing large transient commands. To minimize unacceptable transient commands during FTMAP disengagement, the throttle is left in the position in which it was during FTMAP engagement and the stick is returned to the zero command position. In simulator studies, it was observed that this procedure resulted in noticeable transients only in the longitudinal axis during a high-g turn. This is because the PCS had an essentially full-aft stick command suddenly replaced by a neutral position stick command. The effect was to return the elevator and elevon rapidly from an extreme trailing-edge up position to a zero position. Hence, the vehicle began immediately to lose altitude. The induced transient, while noticeable, was extremely benign and did not require excessive pilot attention to return the vehicle to wings-level flight.

FTMAP Operational Mechanization

The cockpit input panel (fig. 28) allows selection of maneuver and test condition parameters by means of the thumbwheel switches. This panel also includes electromagnetic switches that control FTMAP engagement (level cruise) and maneuver initiation. All commands to the FTMAP return a positive indication when accepted by the autopilot. Because the control switches are magnetic, they can only be engaged (and remain engaged) if the appropriate signals are sent from the FTMAP computer. After the FTMAP is engaged using the level-cruise switch, one of the three status lights on the instrument panel (fig. 27) is illuminated, indicating the current maneuver phase of the FTMAP.

The FTMAP computer continuously monitors a PCS computer-generated disengage signal and a downlink discrete signal that indicates backup control system (BCS) operation. If either of these are set, the FTMAP computer does not permit engagement. An electromagnet is used to hold the two control switches in the engaged position. As a safety precaution, the maneuver switch cannot be engaged if the level-cruise switch is not engaged. The maneuver switch is also equipped with a channel guard to prevent accidental engagement.

The thumbwheel switches (figs. 25 and 28) are used to select the desired maneuver, target condition, and Mach number. The first set of thumbwheel switches defines the maneuver to be performed. Table 1 gives a description of each maneuver by maneuver setting number.

The second set of thumbwheel switches defines (1) the target angle of attack α_{cmd} for either a right or left angle-of-attack commanded windup turn, or (2) the requested angle-of-attack range $\Delta\alpha$ for either type of pushover-pullup maneuver. The third set of thumbwheel switches defines (1) the target normal acceleration for a right or left normal-acceleration commanded windup turn, or (2) the Δa_n for

the rocking-horse maneuver. The fourth set of thumbwheel switches is used to input the Mach number to be reached and maintained during a maneuver.

The LED annunciators display the current thumbwheel switch values registered in the FTMAP computer. The annunciators display only the information pertinent to the selected maneuver. For example, if a normal-acceleration commanded windup turn is selected, a nonzero target angle-of-attack command registers as zero on the LED annunciators.

To monitor FTMAP operation, the cockpit is equipped with three FTMAP status lights located on the instrument panel directly below the attitude-direction-rate and yaw-rate indicators (fig. 27). These lights are horizontally placed LEDs that indicate the present phase of the FTMAP operation. The LEDs indicate (from left to right) level cruise, maneuver, and exit, corresponding to the straight-and-level, maneuver control, and maneuver disengagement phases, respectively.

APPENDIX B — CONTROL LAW DESCRIPTION

The FTMAP control laws are composed of several control modes: altitude hold, angle-of-attack control, normal-acceleration control, wings-level control, turn control, and throttle control (ref. 5). Depending on the maneuver being executed, various modes are selected as shown in table 2.

The altitude-hold mode (fig. 29) maintains altitude during straight-and-level flight. In this mode, the longitudinal command to the aircraft is controlled by an altitude-rate feedback signal and an altitude error signal. The altitude error signal is the difference between the FTMAP engagement altitude and the actual aircraft altitude. The altitude-hold mode is designed to capture altitude under relatively favorable conditions; the combined altitude-rate and altitude error signal is limited to keep the aircraft within the range of 0 to 2.5 g. The limited command signal is multiplied by a gain based on dynamic pressure and is passed through an inverse stick shaper and output limiter.

The angle-of-attack control mode (fig. 30) provides control of the longitudinal axis in the angle-of-attack commanded windup turn and pushover-pullup maneuvers. This mode is based on an angle-of-attack error signal, which is the difference between the commanded FTMAP angle of attack and the sensor-measured angle of attack of the aircraft. The angle-of-attack error signal follows two paths — a direct gain path and an integral gain path. The direct gain path provides an immediate output command but goes to zero as the target condition is reached. The output command produced through the integral path lags the error signal but can maintain a target condition even after the error signal has gone to zero. Saturation of the integrator is prevented by limiting the integrator. The direct path and integral path signals are combined, and the resultant command is passed through a dynamic-pressure gain schedule, an inverse stick shaper, and an output limiter.

The normal-acceleration control mode (fig. 31) is used with the normal-acceleration commanded windup turn and the rocking-horse maneuver. This mode is identical in every respect to the angle-of-attack control mode previously described, except for its inputs. The main inputs for this mode form a normal-acceleration error signal, which is the difference between the commanded FTMAP normal acceleration and the sensor-measured aircraft normal acceleration.

The wings-level control mode (fig. 32) provides control of the lateral axis of the aircraft in both straight-and-level flight and the pushover-pullup maneuver. Bank attitude is maintained near zero through the use of roll-rate and bank-angle feedback signals, which are scaled before being combined. The resultant signal is passed through a combination of limiters and a limited integrator. The first limiter acts as a rate limit to control the maximum rate of change of the lateral command; the second limiter prevents saturation of the integrator. Dynamic pressure and Mach number are used to provide a scheduled scaling factor prior to the final output limiter.

The turn control mode (fig. 33) provides lateral-axis control during any of the turn maneuvers. A roll-rate error signal, an altitude error signal, and an altitude-rate feedback signal are the primary inputs. The reference altitude is maintained by means of the altitude-rate and altitude error signals. The roll-rate and altitude error signals are used to provide effective bank-angle control. The roll-rate signal is scaled before reaching a washout filter. The washout filter removes steady-state effects and allows the turn to be established for a nonzero roll rate. To prevent excessive altitude error

effects, the altitude signal is passed through a limiter and a scaling factor before being combined with the altitude-rate signal. The altitude-rate signal also follows a direct path and is summed downstream of the limited integrator. The combined limiters and limited integrator are identical to those in the wings-level control mode. Dynamic pressure and Mach number are used to compute a scheduled gain factor before the final limiting process.

The throttle control mode (fig. 34) is used in all FTMAP maneuvers except the pushover pullup with fixed throttle. The equivalent throttle command is derived from the combination of an impact-pressure error signal and an impact-pressure-rate feedback signal. The impact-pressure error signal is the result of the combination of a static-pressure input, a commanded Mach input, and an impact-pressure input. The commanded Mach number is passed through a pressure ratio command schedule and then multiplied by ambient pressure to produce an impact-pressure command $q_{c_{cmd}}$. The difference between the commanded impact pressure and the aircraft-measured impact pressure is multiplied by a constant gain factor before being combined with the impact-pressure error signal. A gain schedule that is dependent on altitude provides a scaling factor for the impact-pressure-rate signal. The scaled impact-pressure-rate signal produces faster equivalent throttle response at high altitudes to compensate for changes in the engine dynamics due to altitude.

Under certain conditions, the FTMAP is capable of commanding afterburner — that is, during the straight-and-level maneuver phase if the Mach number command is 1.00 or greater and during the maneuver control phase of any maneuver that uses throttle control. Both the throttle forward-loop gain K_{ab} and the throttle-rate limiter change as a function of commanded engine state. For equivalent throttle commands within the core engine range (less than 98° of the power lever angle command value PLA_{cmd}), these parameters are 1.0 and 50 deg/sec, respectively; for equivalent throttle commands of 98° of PLA_{cmd} or greater, these values are 0.33 and 10 deg/sec, respectively.

APPENDIX C — FTMAP DEVELOPMENT

The functional capability of the FTMAP is derived from two separate functions — the maneuver command generation and the control laws. The maneuver command generation is a subset of the underlying switching and command generation logic. Any of six basic control laws can be selected through this switching and command logic to control the equivalent of throttle setting and longitudinal and lateral stick displacement. This separation of the command and control functions provides a flexible framework in which additional maneuvers can easily be constructed. The basic control laws were determined using linear analysis and classical design techniques. These control laws were expanded to include nonlinear elements and were evaluated in a high-fidelity, real-time, pilot-in-the-loop simulation environment. This simulation was used not only to fine-tune the control laws, but also to develop the command generation and switching logic.

Reference 6 describes the development of the linear control laws and presents a preliminary mechanization of the FTMAP. In references 7 and 8, the current FTMAP mechanization and control details are explained. The following sections of this appendix describe the development of the FTMAP command generation and control functions and the tools used in their development.

Control Law Synthesis

The FTMAP control laws were developed using real-time, pilot-in-the-loop, 6-degree-of-freedom simulation, supported by sampled-data linear analysis. This work was performed under contract to NASA (ref. 6) and formed the basis of FTMAP. Using nonlinear equations of motion and a full-envelope nonlinear aerodynamic model, the linearized state equations were derived about selected trim points using numerical perturbation. The determination of trim using nonlinear equations and the generation of the linear model were performed by using a computer program to produce the A, B, H, and G matrices for a system of the form

$$\dot{\underline{x}} = A\underline{x} + B\underline{u}$$

$$\underline{y} = H\underline{x} + G\underline{u}$$

where $\dot{\underline{x}}$ is the derivative of the state vector with respect to time; $\underline{x}$, $\underline{u}$, and $\underline{y}$ are conventional notations for state, control, and observation vectors, respectively; and A, B, H, and G are state, control, feedforward, and observation matrices, respectively. These matrices provided the basic linear design models for use in a linear design and analysis program (ref. 9). The PCS control laws for the longitudinal and lateral-directional axes were added to the basic aircraft system models to obtain the complete linear system.

Figures 35 and 36 show the block diagrams for the PCS pitch and roll axes, respectively. While these control laws are nonlinear in general, both axes can be easily linearized for a given flight condition. The main nonlinearities of the pitch axis are in the mechanization of the angle-of-attack and normal-acceleration boundary controllers and in the maximum and minimum value select functions. Because the FTMAP was designed to operate within angle-of-attack and normal-acceleration boundary limits, these functions could be ignored for the FTMAP linear analysis. The nonlinear pitch stick shaping is eliminated from the PCS linear model and is compensated by an inverse stick shaper in the FTMAP longitudinal control laws (figs. 29 to 31). Figure 37 shows the linear model of the HiMAT PCS pitch-axis control laws where only the angle-of-attack feedback gain f_{k_α} must be selected as a function of flight condition. This gain f_{k_α} is equal to zero for Mach numbers less than one.

Because all linear analyses were done at subsonic conditions, this loop does not appear in any of the closed-loop analyses.

The PCS roll axis is much less complicated. With only two gains dependent on flight condition, the control laws are virtually linear. The only modification to the linear model is the elimination of the lateral stick gain K_{PD}, which is compensated for by the incorporation of an inverse function in the FTMAP lateral control laws (figs. 32 and 33). Figure 38 shows the linear feedback model used for the roll axis of the HiMAT PCS, and figure 39 shows the linear model used to represent the yaw axis.

A sampled-data root locus analysis was performed using loop closures to represent the normal-acceleration commanded turn, the angle-of-attack commanded turn, altitude hold, the pushover pullup, and the wings-level lateral mode. The system models used for this analysis consisted of four main subsystem models: onboard systems and vehicle model, transmission model, PCS model, and FTMAP model. The onboard systems and the vehicle were modeled as continuous systems. The transmission model represents pure delay induced by the RPRV loop closure. The PCS and FTMAP were represented as discrete models. All the discrete models were analyzed at the uplink rate of 53.3 Hz, which corresponds to the 18.75-msec cycle time of the ground-based PCS and FTMAP computers.

A block diagram of the linear model used to analyze the normal-acceleration commanded windup turn is shown in figure 40. The state vector of the plant is

$$\underline{x} = [u,v,w,p,q,r,\phi,\theta]^T$$

where u, v, and w are the body axis velocities; p, q, and r are the body axis rates; and ϕ and θ are the Euler bank angle and pitch angle, respectively. The control vector for the normal-acceleration commanded windup turn is

$$\underline{u} = [\delta v_a,\delta r,\delta L]^T$$

where δv_a and δr are the asymmetric elevon and rudder deflections, respectively, and δL represents the combined elevator and symmetric elevon deflection. The output vector used for this maneuver model is

$$\underline{y} = [q,a_n,\dot{h},p,r,a_y]^T$$

where a_n and a_y are the normal and lateral body axis accelerations, respectively, and $\dot{h}$ is the altitude rate. All quantities in $\underline{x}$, $\underline{y}$, and $\underline{u}$ are perturbations about their trimmed values for the steady-state turn.

The block diagram for the angle-of-attack commanded windup turn is shown in figure 41. Both the state and control vectors are the same as for the normal-acceleration commanded turn. However, the observation vector has an additional term:

$$\underline{y} = [\alpha,q,a_n,\dot{h},p,r,a_y]^T$$

where α is the angle of attack.

Figure 42 shows the altitude-hold block diagram. The vehicle state vector is

$$\underline{x} = [u,w,q,\theta]^T$$

and the control input is a scalar δL. The output vector is

$$\underline{y} = [\dot{h},a_n,q]^T$$

The pushover pullup (fig. 43) is an unsteady maneuver for which linear analysis at a single flight condition is

not strictly valid. However, closing the angle-of-attack loop at the initial flight condition provided adequate modeling. The state vector for the pushover pullup is the same as that used for the altitude-hold model:

$$\underline{x} = [u,w,q,\theta]^T$$

The control is also the same and is the combined input of elevator and symmetric elevon deflection δL. The observation vector for the pushover-pullup maneuver is

$$\underline{y} = [\alpha,a_n,q]^T$$

The wings-level mode shown in figure 44 is the lateral-directional portion of straight-and-level control and the pushover pullup. For these maneuvers, longitudinal control is modeled by the altitude-hold and pushover-pullup modes, respectively. However, unlike the turn mode, these maneuvers can be easily decoupled into simpler models that can be analyzed separately. The state vector for the wings-level mode is

$$\underline{x} = [v,p,r,\phi]^T$$

and the control vector is

$$\underline{u} = [\delta v_a,\delta r]^T$$

The output vector is

$$\underline{y} = [p,r,a_y,\phi]^T$$

From the linear analysis, five of the six basic control laws were derived: altitude-hold control, angle-of-attack control, normal-acceleration control, wings-level control, and turn control. The respective block diagrams of these control laws are shown in figures 29 to 33. The altitude-hold mode (fig. 29) is derived from the altitude-hold model (fig. 42). The normal-acceleration commanded turn model produced the normal-acceleration control mode (fig. 31). The angle-of-attack commanded turn analysis resulted in the angle-of-attack control mode (fig. 30), which is identical in structure to the normal-acceleration command mode. The turn control mode (fig. 33) was determined from the roll axis of the turn analysis models (figs. 40 and 41) and is the result of design using both normal-acceleration and angle-of-attack command models. The analysis and design using the pushover-pullup model (fig. 37) produced control laws identical to the longitudinal control laws that resulted from the analysis and design of the angle-of-attack commanded turn. Therefore, the angle-of-attack control laws derived from the turn design (fig. 30) could be used to control angle of attack for the pushover pullup. The wings-level control laws (fig. 32) were derived from the wings-level model (fig. 44).

The inverse stick shaper given in all longitudinal control laws (figs. 29 to 31) and the lateral gain factor given in the lateral control laws (figs. 32 and 33) are the results of the modeling technique used to develop the linear models of the PCS pitch and roll axes. Neither of these functions was incorporated into the linear models; therefore, the inverses of those functions were required in the nonlinear FTMAP control laws. Except for the altitude-hold mode, which has no integrator, all control laws contain a limiting function attached to a forward-loop integrator. These functions are added to the system to prevent saturation of the integrator beyond its output capability. Without these limiters on the integrators, large command signals could be built up if the input error signal remained nonzero after the output reached its maximum.

The limits imposed on altitude error and altitude-rate error feedback in the turn control mode (fig. 33) are to prevent saturation of the roll axis caused by large errors in those parameters. The rate-limiting function preceding the forward-loop integrator in the two roll-axis control modes (figs. 32 and 33)

minimizes the transients in output command during mode or command transitions. These nonlinear elements were added to the linear control laws, which were then implemented on the FTMAP computer of the real-time simulation of the HiMAT system.

Simulation Analysis

Control laws (ref. 6) provided by the contractor, Teledyne Ryan Aeronautical Corp., were implemented in the NASA Ames-Dryden simulation facility for evaluation and fine-tuning in a realistic, pilot-in-the-loop environment. The HiMAT-FTMAP simulation system (fig. 45) then replaced the linear analysis program as the FTMAP development tool. The simulation system, which includes the simulation computer, actual flight hardware, and duplicate RPRV facility flight support computers, realistically reproduces the interfaces and timing of the actual RPRV flight system.

Simulation Facility

The simulation computers, consisting of two general-purpose minicomputers and an array processor, model the vehicle aerodynamics and all onboard systems except those modeled in the flight hardware rack. The flight hardware rack consists of a breadboard version of the actual HiMAT onboard computer, an uplink encoder hardlined to a receiver and decoder system (bypassing only the transmitter-receiver radiofrequency link), and high-fidelity electronic models of each of the HiMAT servoactuators. The patch bays serve as general-purpose simulation facility interfaces and route the discrete and analog signals throughout the facility. These patch bays interconnect the simulation computers not only to the flight hardware rack but also to the cockpit through the cockpit-interface electronics.

The simulation facility cockpit is an exact duplicate of the actual flight control cockpit in the RPRV facility. The stick computer is a special-purpose analog computer that controls the force and feel characteristics of the stick. Both the stick computer and the cockpit-interface electronics duplicate the equipment used in the RPRV facility. The simulation facility RPRV computers consist of four minicomputers that are entirely software compatible with the actual RPRV flight computers. The decommutation computers decode the downlink from the simulation computers and select parameters for use in the PCS computer and the FTMAP computer. This system is designed to provide a detailed and highly accurate model of the system illustrated in figure 8 and discussed in the HiMAT systems description in the main body of this report and FTMAP operational characteristics section of appendix A.

The array processor contains a nonlinear model of the HiMAT aerodynamics (including flexibility effects) that covers the entire HiMAT flight envelope. The equations of motion are integrated within the array processor at a 4.54-msec rate using a modified second-order Runge-Kutta integrator. This integration interval corresponds to the 220-Hz downlink rate of the actual flight system (fig. 4). The main simulation computers provide an interface between the array processor and the other simulation equipment. These computers also contain the real-time input-output functions: digital-to-analog conversion, analog-to-digital conversion, and processing of input and output discrete signals. The main simulation computers model the performance of the HiMAT integrated propulsion control system (ref. 10) and engine as a function of throttle setting and flight condition, the atmosphere, onboard instrumentation, and vehicle sensors. The use of this HiMAT simulation to develop and qualify ground-based flight codes such as the FTMAP is discussed in reference 11.

Development of Throttle Control Mode

Using the real-time simulation, the FTMAP throttle control mode (fig. 34) was developed on the basis of the BCS high-altitude throttle control law. References 12 and 13 describe the BCS in general and the BCS throttle control laws in particular. Impact-pressure rate, derived from an onboard analog differentiation of the output of the impact-pressure sensor (app. D), was essential to the success of the FTMAP Mach-number control.

The BCS throttle control laws were designed for control of the core engine from idle to military power. However, the FTMAP was also required to control the afterburner. Several modifications to the basic control laws were needed to accommodate this expanded range of operation. Two changes of a generic nature were required; that is, the forward-loop gain K_{ab} was lowered, and the throttle-rate limit was decreased in the afterburner command range. Both of these changes were based on predictions from a batch simulation of the HiMAT J85-21 engine performance, such as that illustrated in figure 46. Both variables, K_{ab} and throttle-rate limit, are related to the slope of the thrust curve. Because this slope is a factor of two or three larger for the afterburner region than for the core region, the two parameters were reduced accordingly.

Another change to general throttle control was based on the predicted thrust differential between military and minimum afterburner. A timer was added to eliminate a potential cycling in and out of the afterburner in the windup turn that might be caused by this thrust differential. This timer prevents a return to the core engine region for 5 sec following an afterburner request. This allows the angle-of-attack or normal-acceleration commanded control law the necessary time to increase the commanded parameter sufficiently to raise thrust demand above that provided at minimum afterburner.

Development of Command Generation Function

The HiMAT-FTMAP simulation system was also used extensively to develop the command generation functions (fig. 25) required to support the automatic maneuvers. The maneuver command generation function can be used to specify the commanded angle of attack, normal acceleration, bank angle, roll rate, altitude, altitude rate, and Mach number.

In all the FTMAP maneuvers, commands were generated to control the time-varying parameters. These commands were based on the selected maneuver and the target conditions input on the thumbwheel switches. The angle-of-attack command is used during the pushover-pullup maneuvers and the angle-of-attack commanded windup turns. Normal-acceleration command is used during the normal-acceleration commanded windup turns and the rocking-horse maneuver. During the windup turns, the angle-of-attack and normal-acceleration commands increase linearly at a specified command rate.

The command rates for the HiMAT program are currently set at 0.25 deg/sec for angle of attack and 0.2 g/sec for normal acceleration. The command is ramped from the trimmed value to the target condition. When the throttle control first commands the afterburner region, the angle-of-attack and normal-acceleration commands are slowed to allow time for a stable afterburner light and the attendant increase in thrust before continuing. This 2-sec delay prevents excessive thrust demand and subsequent Mach loss during afterburner lighting. Angle-of-attack and normal-acceleration commands are also used during the exit phase of the turn and rocking-horse maneuvers. During the

exit phase, the commands are ramped down to the initial trim condition at the previously described command rates.

The angle-of-attack command for the pushover-pullup maneuver is illustrated in figure 5, where $\Delta\alpha$ corresponds to the value $\Delta\alpha_{cmd}$ requested on the second set of thumbwheel switches. Starting at the trim value, angle-of-attack command is linearly decreased to $\alpha - \alpha_{cmd}$. When the minimum value is reached, the command is held for a specified time Δt_α. The command is then linearly ramped until it is $\Delta\alpha_{cmd}$ above the trim value. This new value is held for Δt_α seconds, and then the angle of attack is linearly ramped back to its original trim value. Both the command rate and the hold time are variable from flight to flight by means of a software change. The final values were 0.50 deg/sec for the angle-of-attack command rate and 0 sec for the hold time.

The rocking-horse maneuver is controlled with the normal-acceleration command. The windup turn to the zero-excess-thrust condition is the same as the normal-acceleration commanded windup turn, except for the region where the equivalent throttle command approaches maximum afterburner. The normal-acceleration command rate is reduced from 0.2 g/sec at 80-percent full equivalent throttle to 0.02 g/sec at 95-percent and above full equivalent throttle (fig. 47). The command reduction is based on percent equivalent throttle to allow the rocking-horse mode to be exercised during conditions other than maximum afterburner. On the simulator, this slowing of the command rate has proven very effective in simultaneously approaching zero-excess-thrust normal acceleration a_{n_o} and maximum afterburner command. In fact, this technique has eliminated the need to adjust the final a_{n_o}. During the rocking-horse maneuver, the throttle command is locked at the predefined zero-excess-thrust throttle setting. Although the option of performing a rocking-horse maneuver at various throttle settings was available, only the maximum afterburner setting was used.

In the turning maneuvers, bank-angle command was set to 0° and was not used for maneuver control. Originally, this command was used for turn initiation. Roll-rate command was later used to initiate the roll into the turn. This command was set to 10.00 deg/sec and was maintained until the vehicle had achieved a 35° bank angle. At that time, the roll-rate command was set to 0 deg/sec.

For all conditions except the thrust-limited windup turn, altitude and altitude-rate command are not used dynamically; that is, altitude reference is set to the vehicle altitude at PTMAP engagement, and altitude-rate command is zero. However, for the thrust-limited windup turn, reference altitude tracks the current vehicle altitude, and altitude-rate command is based on Mach-number error (fig. 48). The integral path commands a steady-state altitude rate, limited to -3020 m/min (-10,000 ft/min). The direct path can provide a quick nose-down roll into the thrust-limited maneuver to prevent excessive Mach error. The altitude-rate command mode is activated when the zero-excess-thrust condition is detected during a windup turn.

Mach number is normally commanded directly from the thumbwheel switches. However, for some of the maneuvers, negative or positive increments are added to the selected reference Mach number M_{ref} to aid Mach control. During the straight-and-level phase of all turning maneuvers, an increment of 0.01 Mach is added to M_{ref}. This value is held until the zero-excess-thrust condition is reached, at which time the increment is set to 0.02 Mach to increase the commanded altitude rate. Artificially increasing the target Mach

number provides sufficient lead time to allow the engine or the aircraft to respond to a known future requirement. When the exit phase is initiated, the increment is eliminated. This same approach has led to the somewhat more involved method used in the constant-Mach pushover pullup. For this latter maneuver, an increment of -0.01 Mach is added to M_{ref} during the straight-and-level portion of the maneuver. As the decreasing angle-of-attack command begins, this adjustment is set to 0.01 Mach and held constant until the minimum angle of attack is reached. The Mach increment is then reset to zero.

Switching logic within the FTMAP is used for several purposes: (1) to change between the three maneuver phases, (2) to detect zero excess thrust in the windup turns, (3) to change to the thrust-limited turn, (4) to determine when to initiate each portion of the rocking-horse maneuver, and (5) to provide the anticipated throttle commands. The switching logic is functionally interrelated to the command generation, but conceptually it can be treated separately. Use of a full-envelope nonlinear simulation was essential in the development of the switching logic, for which the HiMAT-FTMAP simulation system was used extensively.

At FTMAP engagement, the altitude-hold (fig. 29), wings-level control (fig. 32), and throttle control (fig. 34) modes are used to command the vehicle to a straight-and-level condition at the reference altitude and requested Mach number. The forward-loop integrator of the throttle control mode is initialized to the pilot commanded cockpit throttle position. The forward-loop integrator in the wings-level control mode is initialized to zero. No signal ramping is performed in any axis. Because of its initialization, the throttle control engagement is transient-free. The engagement of the other two axes is transient-free only if the FTMAP is engaged when the vehicle is straight and level. The effects of off-nominal engagement of the FTMAP are illustrated in figure 49. This simulation operated at a 7600-m (25,000-ft) altitude and Mach 0.90 shows an off-condition engagement at extreme conditions. The altitude rate is in excess of 30 m/sec (100 ft/sec), and roll attitude is approximately 40°. At FTMAP engagement, the FTMAP longitudinal command is a stick forward step, resulting in the 3.00- to 5.00-deg/sec angle-of-attack rate. There is a small roll-axis transient, but the effects of the wings-level control mode can be seen on the bank-angle trace, where a wings-level condition is achieved in 4 sec and is completely damped in 6 sec.

When a maneuver is commanded, the straight-and-level phase is continued for 5 sec to ensure straight-and-level flight. The longitudinal command is switched from the altitude-hold mode (fig. 29) to the appropriate command mode — that is, either the normal-acceleration (fig. 31) or the angle-of-attack (fig. 30) control mode. The lateral-axis control is switched from the wings-level mode (fig. 32) to the turn control mode (fig. 33) when a turn is requested; otherwise, the wings-level mode is used throughout the maneuver. The mode switching in the pitch axis is transient-free because α_{cmd} (fig. 30) or $a_{n_{cmd}}$ (fig. 31) is initialized to the straight-and-level value of the corresponding parameter, and because the forward-loop integrators are initialized to the output of the altitude-hold mode (scaled appropriately to account for the inverse stick shaper and the dynamic-pressure scheduled gain). The transition from the wings-level mode (fig. 32) to the turn control mode (fig. 33) is minimized because the turn control integrator is initialized to the value of the wings-level control integrator, and because the washout filter on roll-rate feedback is initialized to the zero-roll-rate error condition.

To initiate the turn, a roll-rate command is used to achieve a 35° bank angle ϕ. At ϕ equal to 35°, the command is set to zero. Figure 49 shows the virtually transient-free nature of this mode switching into the maneuver. The transition from the maneuver phase to the exit phase of a maneuver involves no mode switching and always terminates with a 2-sec linear ramping between the output of either the normal-acceleration or the angle-of-attack control mode and that of the altitude-hold mode. The transition from the exit phase back to the straight-and-level phase begins when the command parameter has returned to the initial trim value. At that point, the previously described longitudinal ramping begins, and the lateral control mode is switched to the wings-level mode if the aircraft is coming out of a turn.

The logic to detect the zero-excess-thrust condition was perhaps the most difficult of all developments for the FTMAP. Various approaches, such as directly computing the specific power P_s and calculating the total vehicle acceleration $\dot{V}$, were tried. However, a simple scheme was ultimately used. Velocity was monitored 0.2 sec after maximum afterburner was commanded. If velocity decreased consistently for 0.1 sec (six computational cycles), a thrust-limited condition was declared. This technique was used for both the normal windup turns and the turn into the rocking-horse maneuver without a false thrust-limited condition being declared.

During the normal windup turns, detection of zero excess thrust results in the engagement of the altitude-rate command mode (fig. 48). In thrust-limited turns, the transition to the thrust-limited condition results in a step input to the altitude-rate command (fig. 48), which in turn, causes a step input into the turn control mode (fig. 33). Two factors cause this response — the Mach number is usually below the target Mach as the zero-excess-thrust condition is approached, and a Mach increment is added to M_{cmd} (fig. 48), as described previously in this appendix. This step results in an abrupt altitude-rate command, which bypasses the forward-loop integrator in the turn control mode (fig. 33). A rapid increase in bank angle results, and because the bank angle is more than that required for level flight with the commanded normal acceleration, the vehicle begins a downward spiral and quickly acquires the velocity necessary to maintain the target Mach number.

Flight Test Development

Use of the HiMAT-FTMAP simulation did not end when FTMAP flight testing began. In fact, the simulator became even more important during this part of the FTMAP development and served to minimize the problems encountered during flight. The simulation was used not only to develop and qualify every modification mode for the FTMAP, but also to plan each mission prior to flight. This allowed potential FTMAP problems to be detected in the simulation rather than in flight. In addition, the simulation was used as a diagnostic tool. For difficulties encountered in flight, the simulator could often be used for duplication, analysis, and correction of the problem. For example, the dynamic-pressure gain scheduling in the FTMAP longitudinal control modes resulted from such a process. The pitch axis seemed to have too little damping during flight at high dynamic pressures. However, by increasing the forward-loop gain to decrease the gain margin in the pitch axis, the problem was duplicated reasonably well on the simulator. The gain schedule was then developed and tested using the simulation before flight test.

Experience with the original design of the turn initiation command for windup turns involved a different set of problems. The original design (ref. 6) used a nonzero bank-angle command to

initiate the roll into the windup turns. The roll into the turn was assisted by a bank-angle command that remained in effect from turn initiation until the bank angle was within 10° of the commanded bank angle. After being qualified on the real-time simulation, this scheme was used on the first two maneuvering flights.

Figure 49 shows the results of a simulated windup turn at an altitude of 7600 m (25,000 ft) and Mach 0.90. This maneuver was engaged outside the normal capture window with an altitude rate in excess of 1820 m/min (6000 ft/min) and a 40° bank angle, which resulted in a capture with significant equivalent stick activity. Although somewhat less damped than desired in the roll axis for the engagement of the straight-and-level phase, the simulated performance during the turn from maneuver initiation to exit command was excellent.

On the second FTMAP maneuvering flight, a windup turn was attempted twice. As shown in figure 50, the equivalent lateral stick command went from stop to stop on the output limiter of the turn control mode. The flight performance was unacceptable and was also not reproducible on the HiMAT-FTMAP simulation, even with the turn control mode gains raised by a factor of three. On the basis of a review of the roll-axis control techniques used by the pilot, the rate of maneuver initiation (that is, the roll rate at maneuver initiation) was decreased by eliminating the bank-angle command. Thus, the turn command scheme was modified to be a function of roll-rate command to achieve a minimum bank angle. Figure 51 shows the flight results that employed this modified bank-angle command method and illustrates the improved performance.

Although the HiMAT-FTMAP simulation has proven to be a valuable tool, it has significant limitations. The HiMAT systems are represented by highly refined hardware models or even exact duplicates of actual flight systems. However, the key element — the aerodynamic model — has inaccuracies and inherent unknowns that hamper the translation from simulation to flight. Further, the relative inaccessibility of the aerodynamic model in the array processor, combined with schedule constraints, virtually eliminates consideration of aerodynamic variations. A mechanization such as the FTMAP puts more demands on a simulation system than does a pilot or a conventional autopilot. The control loops in the FTMAP are tightly closed to provide precise command tracking. Thus, the FTMAP is somewhat more sensitive to modeling errors than are normal controllers. However, this alone cannot explain all the differences between simulation and flight results. In addition, the effects of these modeling errors could have been minimized in a more flexible simulation that allowed variations in the parameters to which the FTMAP was sensitive. This problem of parameter sensitivity is discussed in the FUTURE RESEARCH section of this report.

APPENDIX D — SPECIAL HiMAT INSTRUMENTATION

In addition to the standard set of flight test instrumentation, the HiMAT vehicle was equipped with onboard electronics that provided two unique parameters that greatly aided the development and application of the FTMAP. These parameters were static-pressure rate and impact-pressure rate. Static-pressure rate was used to compute an altitude-rate signal without the large delays normally associated with altitude-rate measurements. Impact-pressure rate was used directly in the throttle control mode (fig. 34) to provide damping as well as to prevent overshoot in Mach number.

Both signals were derived from normal instrumentation. Each of the onboard static-pressure and impact-pressure signals was differentiated with analog filters whose transfer functions were

$$G(s) = \frac{s}{(0.2s + 1)^2}$$

where s is the Laplace variable. These differentiated analog signals were then digitized and sent to the ground-based computers using the telemetry downlink.

The static-pressure-rate signal was used to compute altitude rate using the measured static pressure and the schedule of static-pressure gradient as a function of altitude shown in figure 52. Figure 53 shows the altitude-rate calculation in block diagram form.

REFERENCES

1. Swann, M.R.; Duke, Eugene L.; Enevoldson, Einar K.; and Wolf, Thomas D.: Experience With Flight Test Trajectory Guidance. AIAA-81-2504, Nov. 1981.

2. Arnaiz, Henry H.; and Loschke, Paul C.: Current Overview of the Joint NASA/USAF HiMAT Program, in Tactical Aircraft Research and Technology, NASA CP-2162, part 1, 1980, pp. 91-121.

3. Petersen, Kevin L.: Flight Control Systems Development of Highly Maneuverable Aircraft Technology (HiMAT) Vehicle. AIAA-79-1789, Aug. 1979.

4. Duke, Eugene L.; and Jones, Frank P.: Computer Control for Automated Flight Test Maneuvering. J. Aircraft, vol. 21, no. 10, Oct. 1984, pp. 776-782.

5. Duke, Eugene L.; Jones, Frank P.; and Roncoli, Ralph B.: Development of a Flight Test Maneuver Autopilot for a Highly Maneuverable Aircraft. AIAA-83-0061, Jan. 1983.

6. Final Report, HiMAT Maneuver Autopilot. TRA 29255-1, Teledyne Ryan Aeronautical Corp., 1981.

7. Roncoli, Ralph B.: A Flight Test Maneuver Autopilot for a Highly Maneuverable Aircraft. NASA TM-81372, 1982.

8. Duke, Eugene L.: Automated Flight Test Maneuvers: The Development of a New Technique. Flight Testing Technology Proc. SFTE, 13th Annual Symposium, New York, Sept. 1982, pp. 101-119.

9. Edwards, John W.: A FORTRAN Program for the Analysis of Linear Continuous and Sampled-Data Systems. NASA TM X-56038, 1976.

10. Bayati, Jamal E.: The HiMAT RPRV Propulsion Control System. SAE 760887, Nov.-Dec. 1976.

11. Myers, Albert: Simulation Use in the Development and Validation of HiMAT Flight Software. AGARD 28th Guidance and Control Panel Symposium, Ottawa, Canada, May 1979.

12. Hoyt, Carl E.; Kempel, Robert W.; and Larson, Richard R.: Backup Flight Control System for a Highly Maneuverable Remotely Piloted Research Vehicle. AIAA-80-1761, Aug. 1980.

13. Kempel, Robert W.: Flight Experience With a Backup Flight Control System for the HiMAT Research Vehicle. AIAA-82-1541, Aug. 1982.

TABLE 1. — MANEUVER SETTINGS

Maneuver setting number	Description of maneuver
1	Normal-acceleration commanded windup turn to the right
2	Normal-acceleration commanded windup turn to the left
3	Angle-of-attack commanded windup turn to the right
4	Angle-of-attack commanded windup turn to the left
5	Pushover-pullup maneuver with throttle fixed
6	Pushover-pullup maneuver with constant Mach
7	Rocking-horse maneuver to the right
8	Rocking-horse maneuver to the left

TABLE 2. — CONTROL MODES USED FOR MANEUVERS

Maneuver	Control mode
Straight and level	Attitude hold, throttle control, and wings-level control
Pushover pullup	Angle-of-attack control, throttle control,[a] and wings-level control
Normal-acceleration commanded windup turn	Normal-acceleration control, throttle control,[b] and turn control
Angle-of-attack commanded windup turn	Angle-of-attack control, throttle control,[a] and turn control
Rocking horse	Normal-acceleration control, throttle control,[b] and turn control

[a]Not used in fixed-throttle maneuver.

[b]Not used after $P_s = 0$ condition.

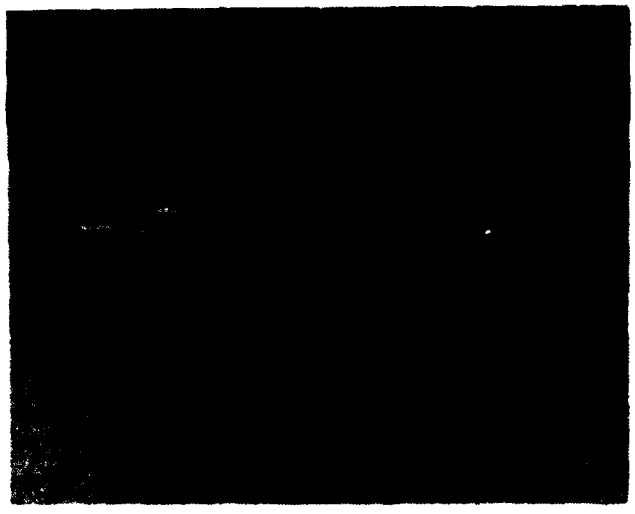

ECN 9954

Figure 1. Himat RPRV on Edwards dry lakebed.

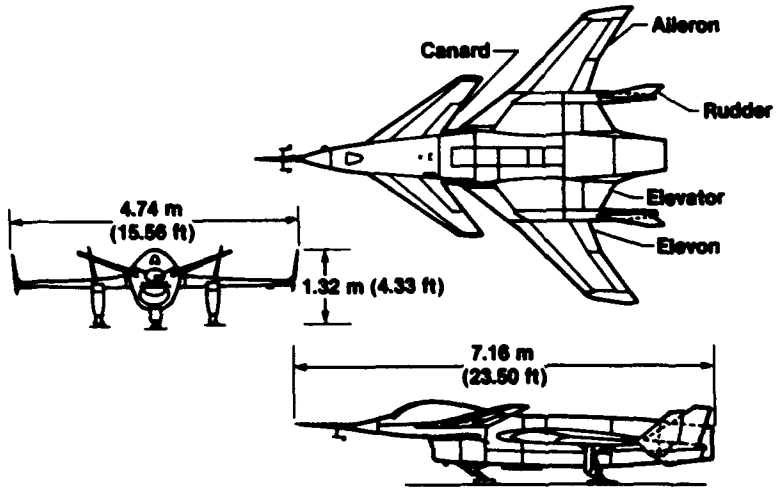

Figure 2. Three-view drawing of HiMAT vehicle.

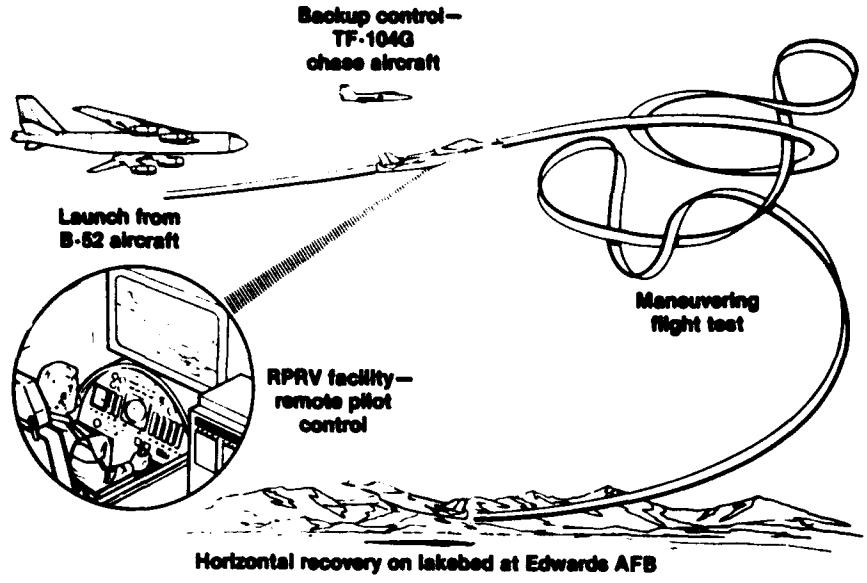

Figure 3. HiMAT operational concept.

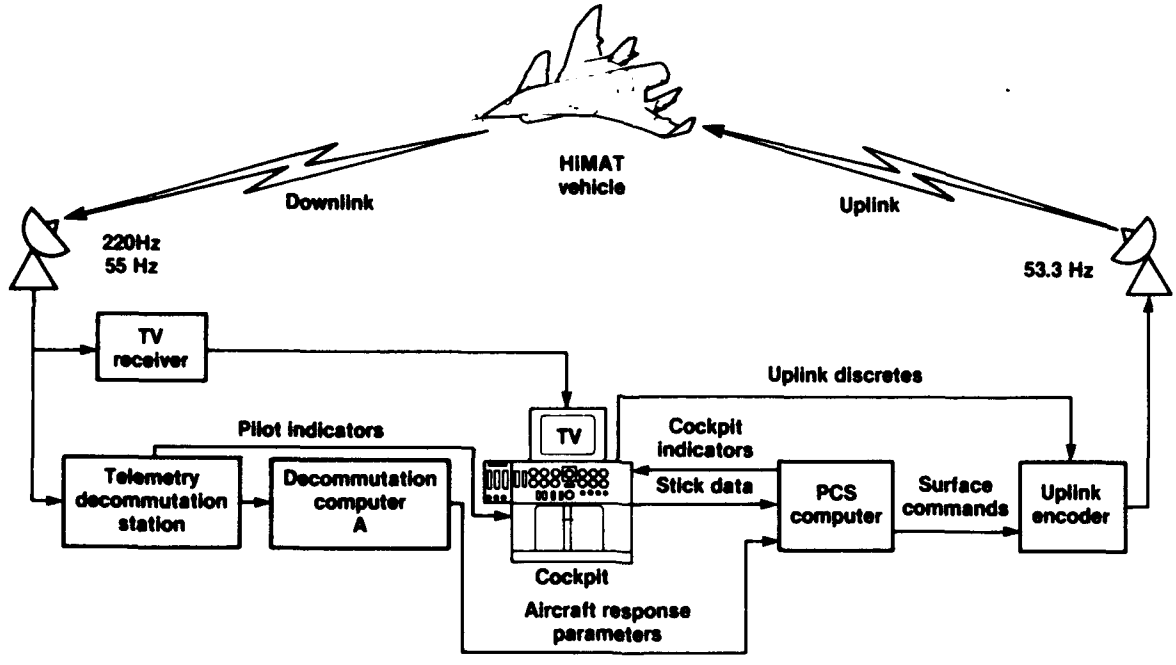

Figure 4. HiMAT RPRV primary control system.

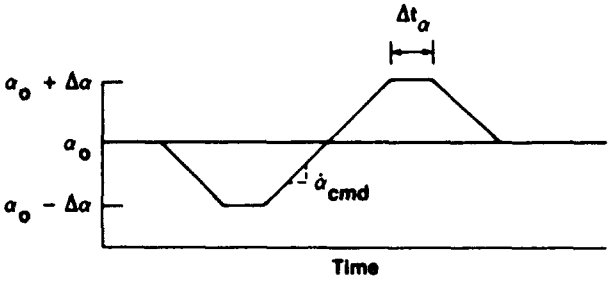

Figure 5. Angle-of-attack command for pushover-pullup manuever.

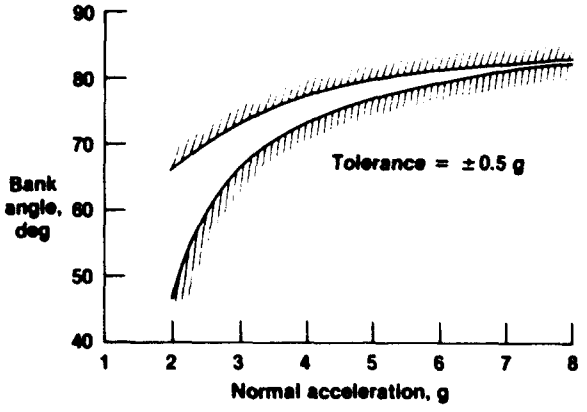

Figure 6. Bank-angle tolerances for level turning flight.

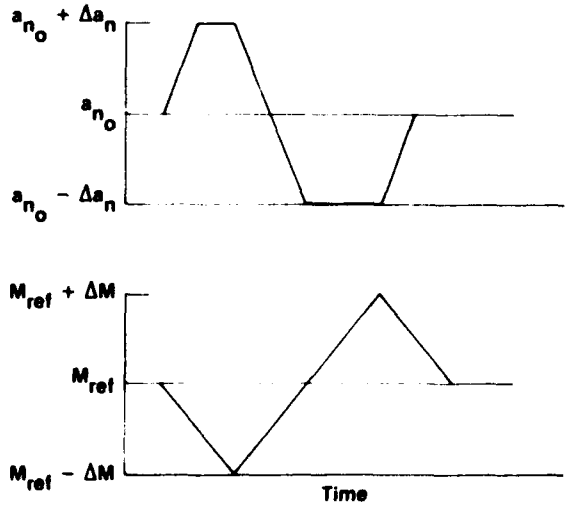

Figure 7. Normal-acceleration command and Mach number response during one cycle of rocking-horse maneuver.

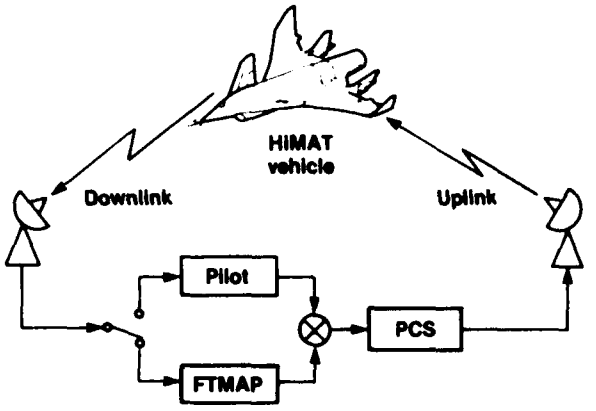

Figure 8. Conceptual block diagram of HiMAT flight system with FTMAP.

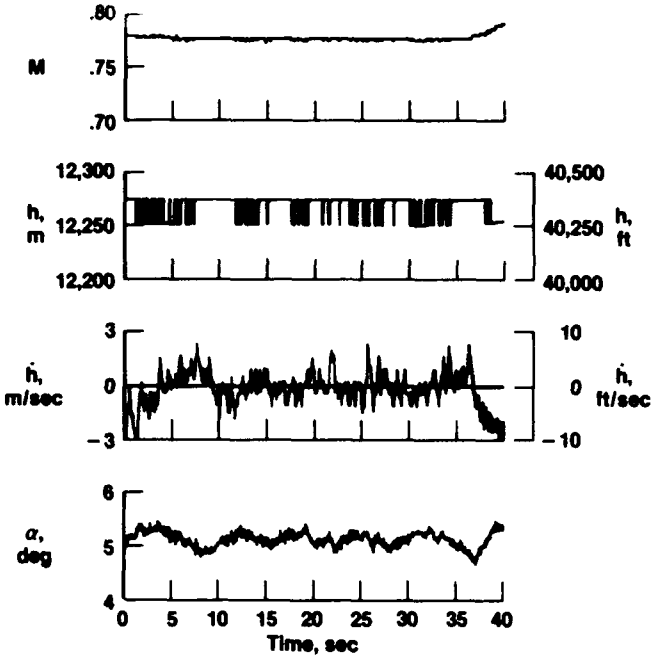

Figure 9. FTMAP constant-altitude, constant-Mach cruise at nominal conditions of Mach 0.80 and 12,200-m (40,000-ft) altitude.

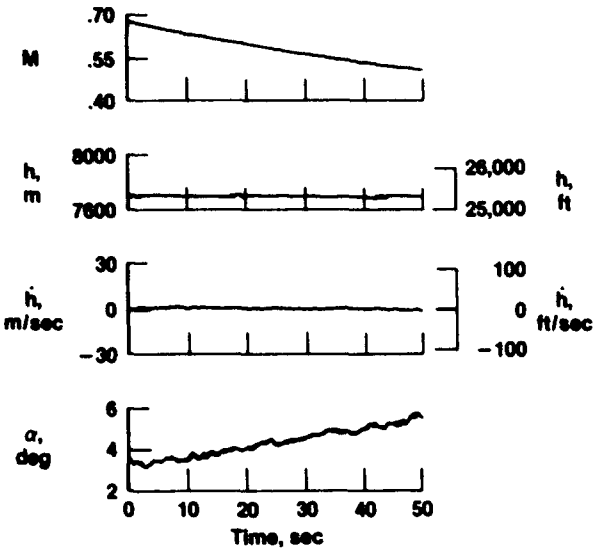

Figure 10. FTMAP constant-altitude deceleration at nominal conditions of Mach 0.70 to 0.50 and 7600-m (25,000-ft) altitude.

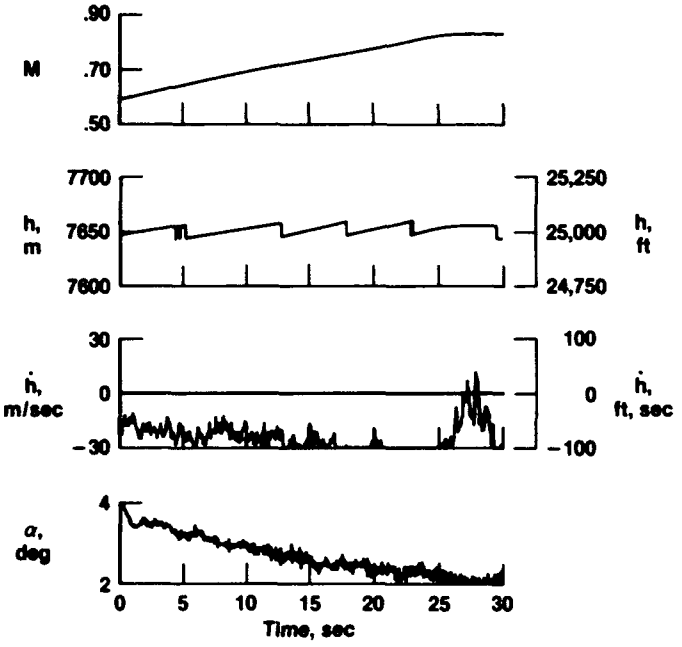

Figure 11. FTMAP constant-altitude acceleration at nominal conditions of Mach 0.50 to 0.80 and 7600-m (25,000-ft) altitude.

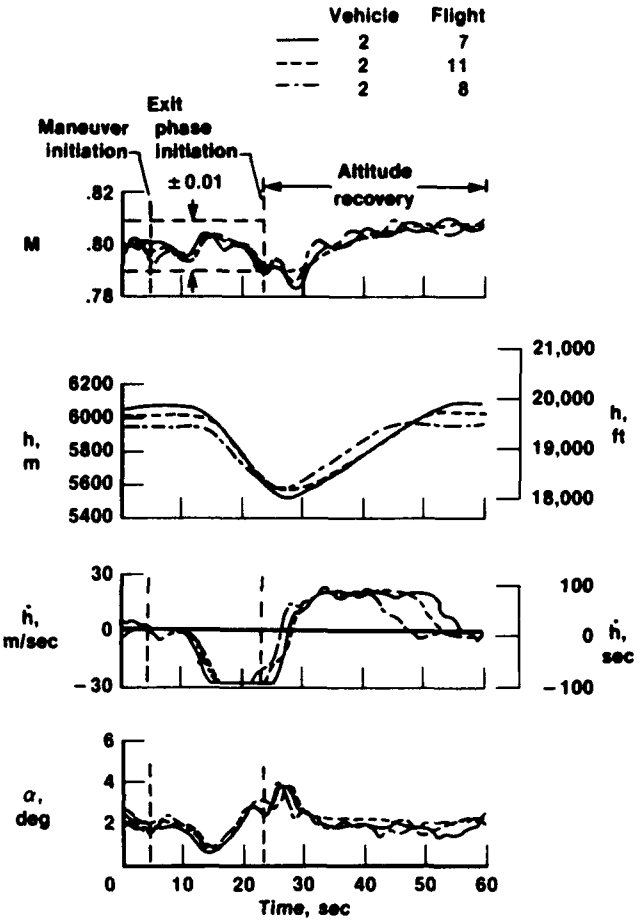

Figure 12. Comparison of three FTMAP pushover-pullup maneuvers at nominal conditions of Mach 0.80 and 6100-m (20,000-ft) altitude.

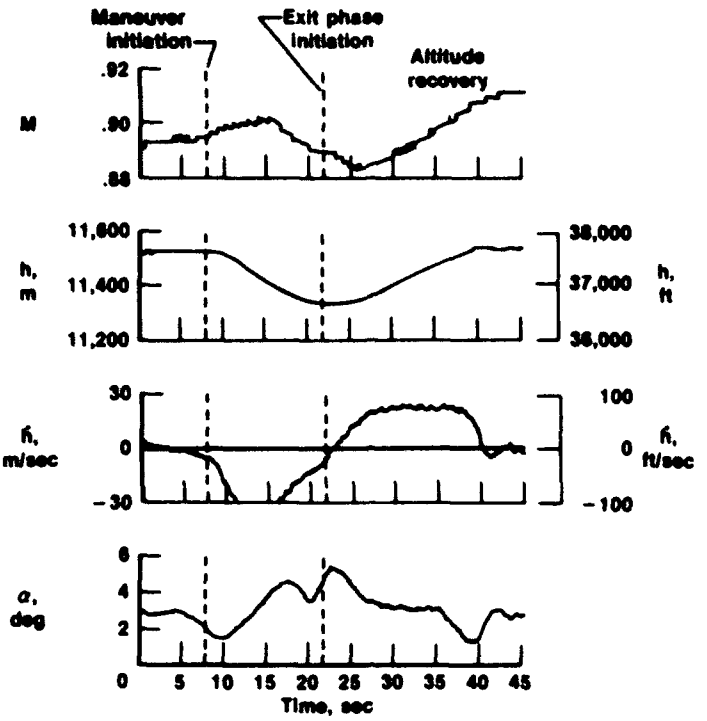

Figure 13. FTMAP pushover-pullup maneuver at nominal conditions of Mach 0.90 and 11,600-m (38,000-ft) altitude.

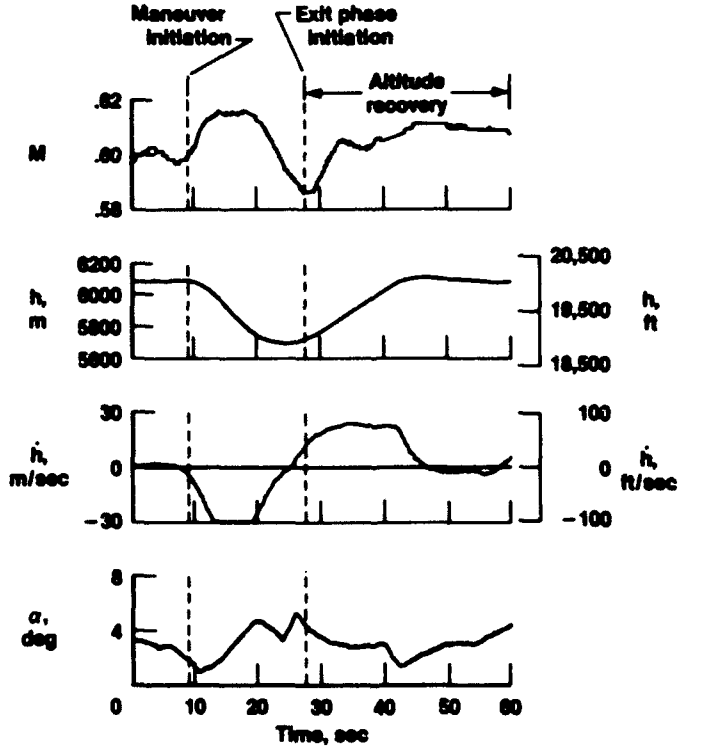

Figure 14. FTMAP pushover-pullup maneuver at nominal conditions of Mach 0.60 and 6100-m (20,000-ft) altitude.

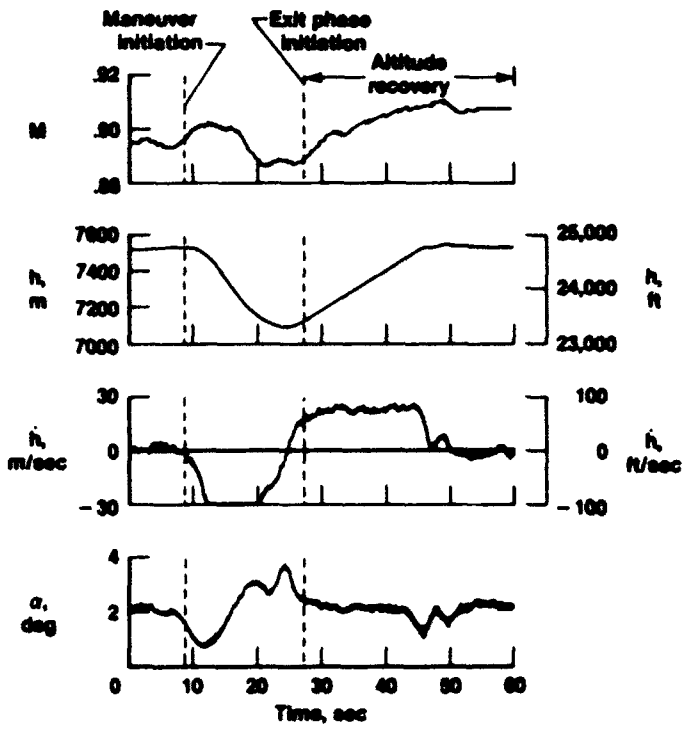

Figure 15. FTMAP pushover-pullup maneuver at nominal conditions of Mach 0.90 and 7600-m (25,000-ft) altitude.

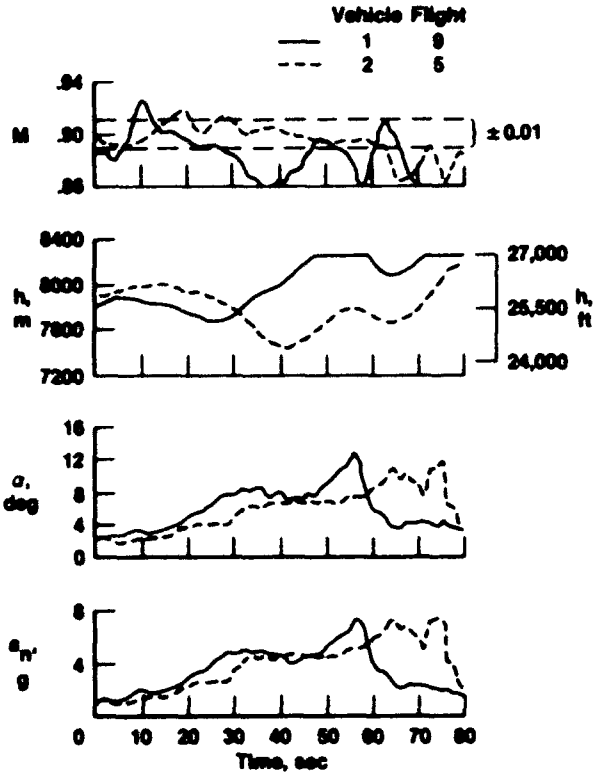

Figure 16. Comparison of two pilot-flown windup turns at nominal conditions of Mach 0.90 and 7600-m (25,000-ft) altitude.

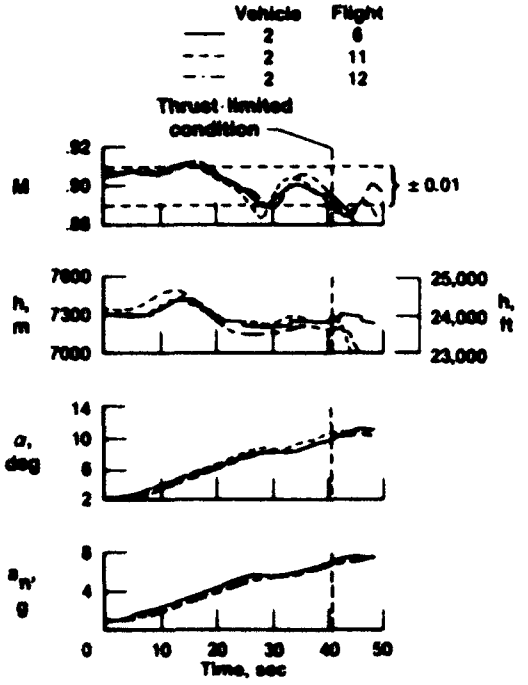

Figure 17. Comparison of three FTMAP-flown windup turns at nominal conditions of Mach 0.90 and 7600-m (25,000-ft) altitude.

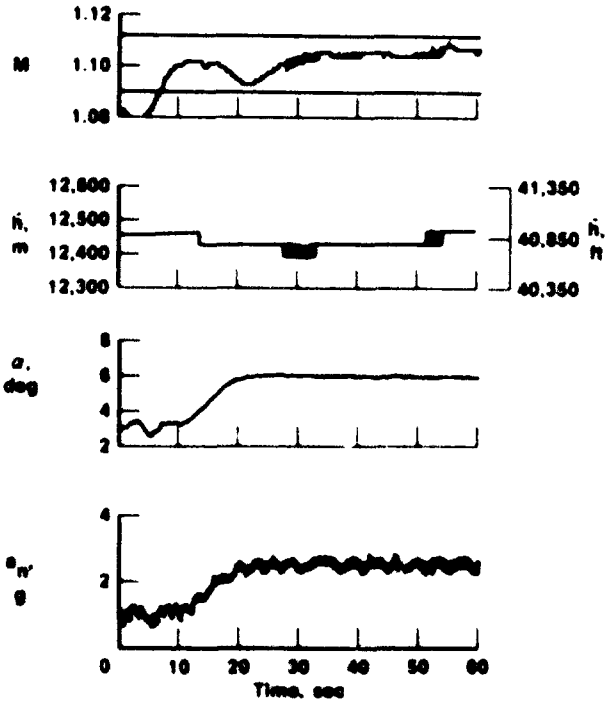

Figure 18. FTMAP supersonic excess-thrust windup turn at nominal conditions of Mach 1.10 and 12,200-m (40,000-ft) altitude.

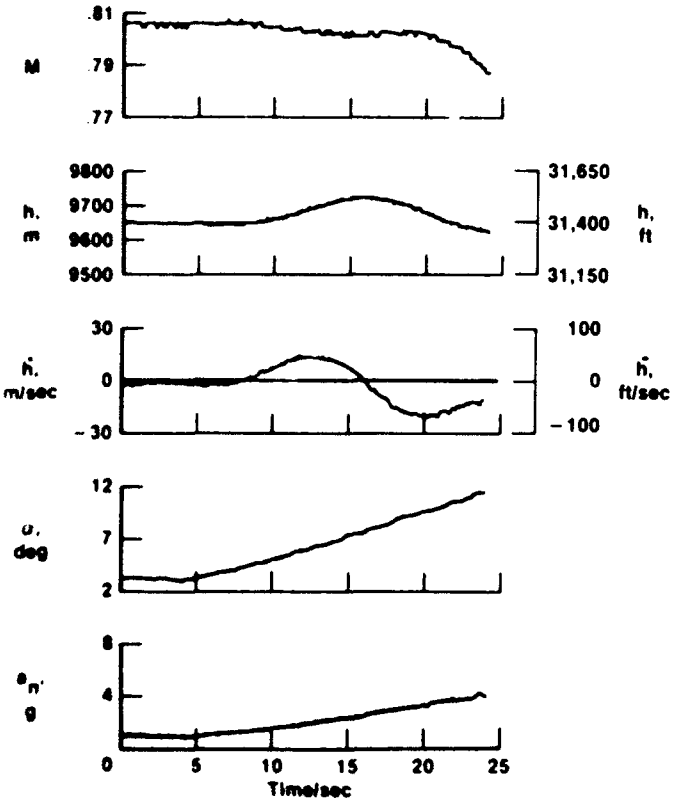

Figure 19. FTMAP windup turn flown within given tolerances at nominal conditions of Mach 0.80 and 9800-m (32,000-ft) altitude.

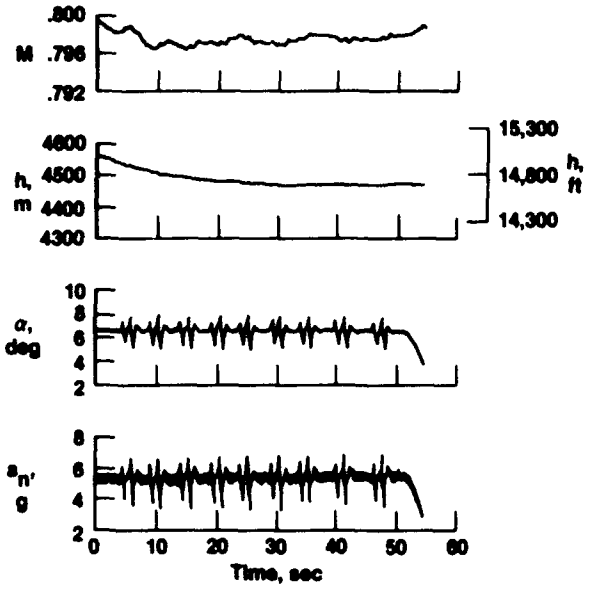

Figure 20. FTMAP steady-state windup with elevator doublets input at nominal conditions of Mach 0.80 and 4600-m (15,000-ft) altitude.

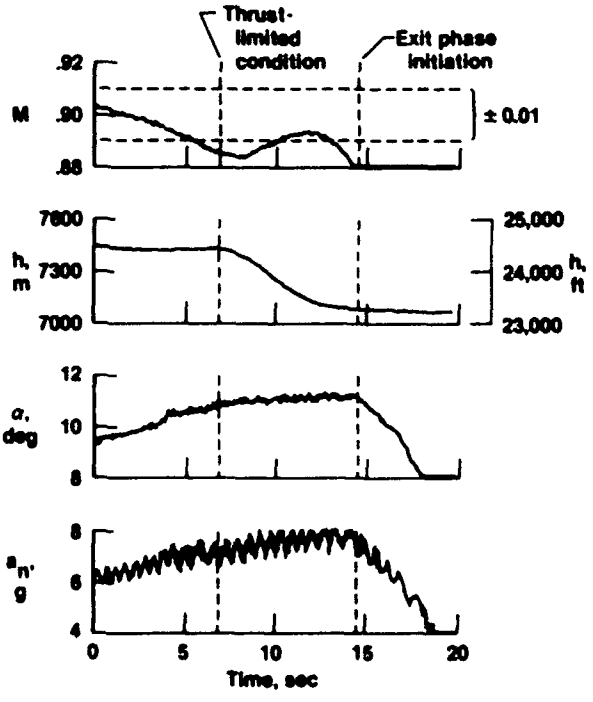

Figure 21. FTMAP thrust-limited windup turn at nominal conditions of Mach 0.90 and a 7600-m (25,000-ft) altitude.

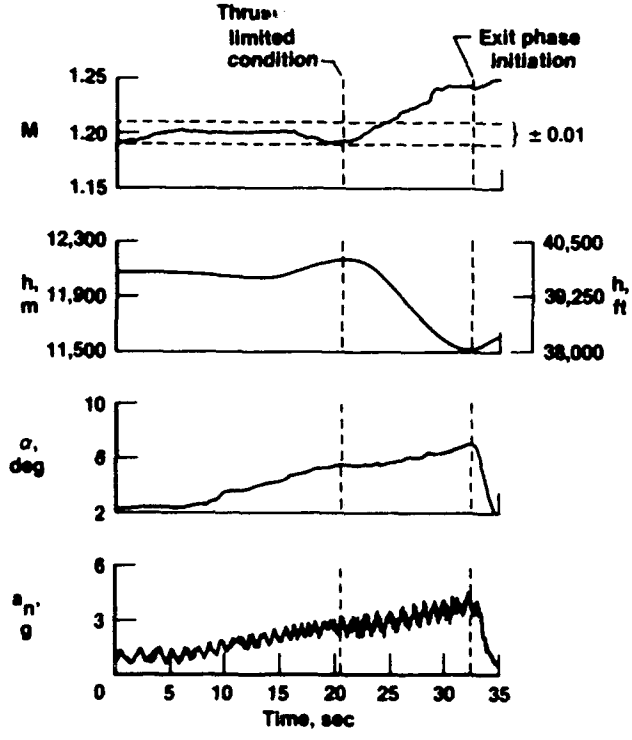

Figure 22. FTMAP supersonic thrust-limited windup turn at nominal conditions of Mach 1.20 and 12,200-m (40,000-ft) altitude.

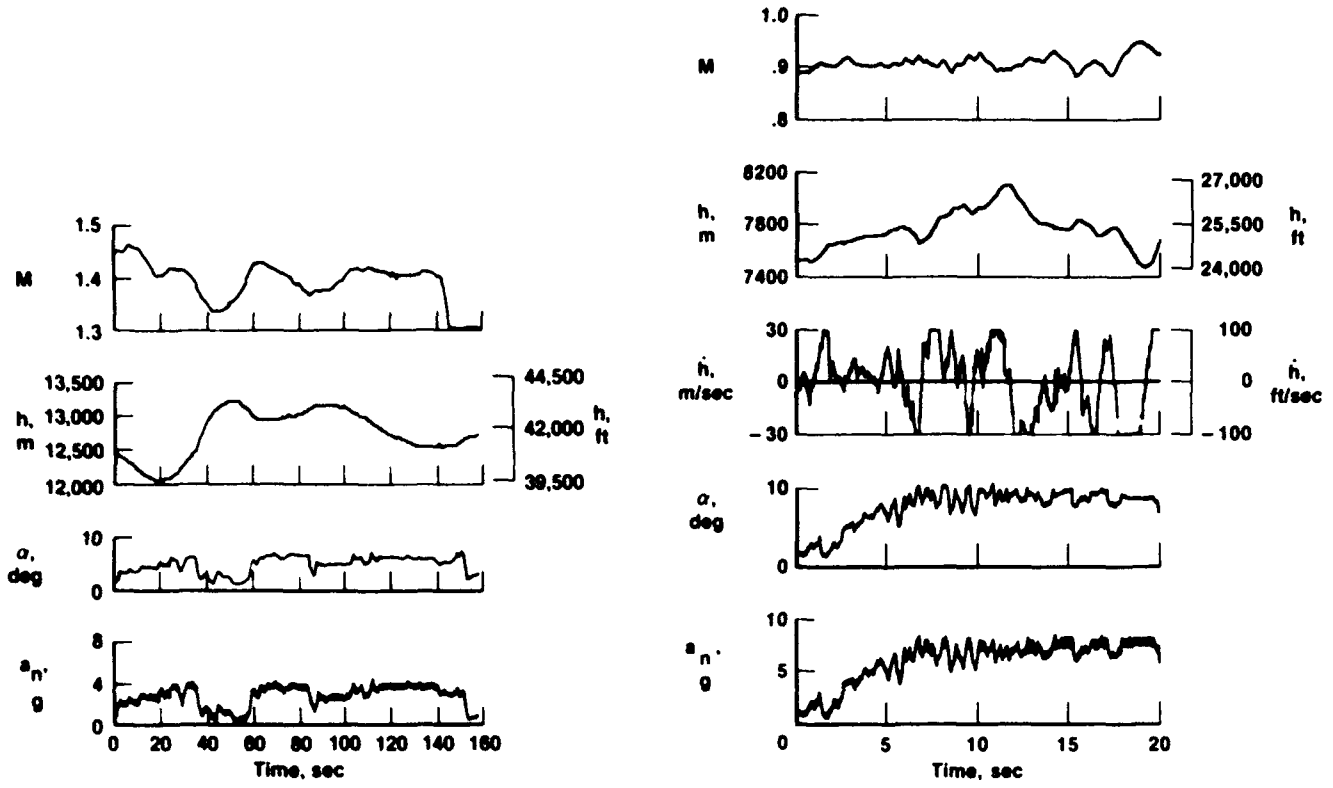

(a) Nominal conditions of Mach 1.40 and 12,200-m (40,000-ft) altitude.

(b) Nominal conditions of Mach 0.90 and 7600-m (25,000-ft) altitude.

Figure 23. Two pilot-flown rocking-horse maneuvers.

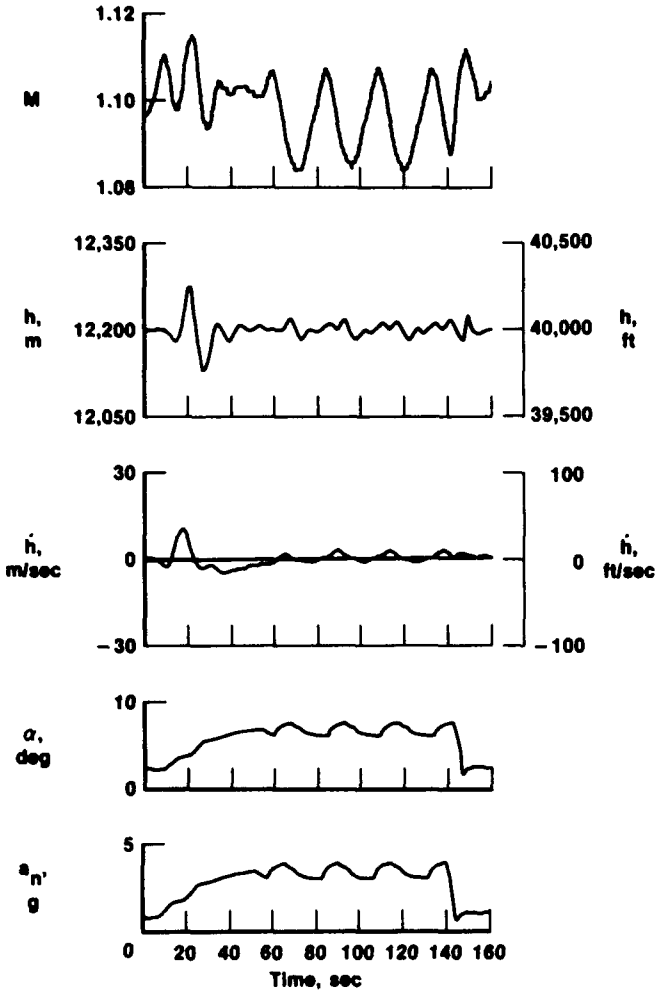

(a) Nominal conditions of Mach 1.10 and 12,200-m (40,000-ft) altitude.

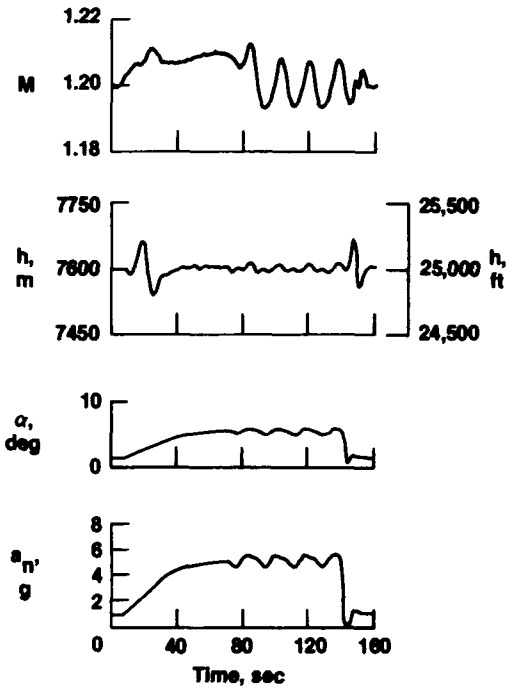

(b) Nominal conditions of Mach 1.20 and a 7600-m (25,000-ft) altitude.

Figure 24. Two simulated FTMAP rocking-horse maneuvers.

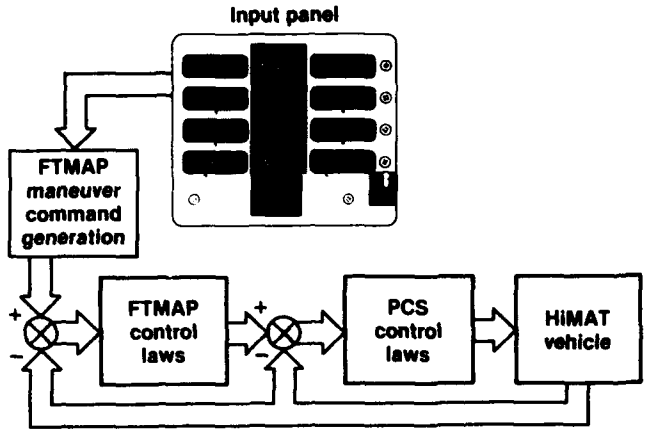

Figure 25. Overview of the FTMAP-HiMAT system.

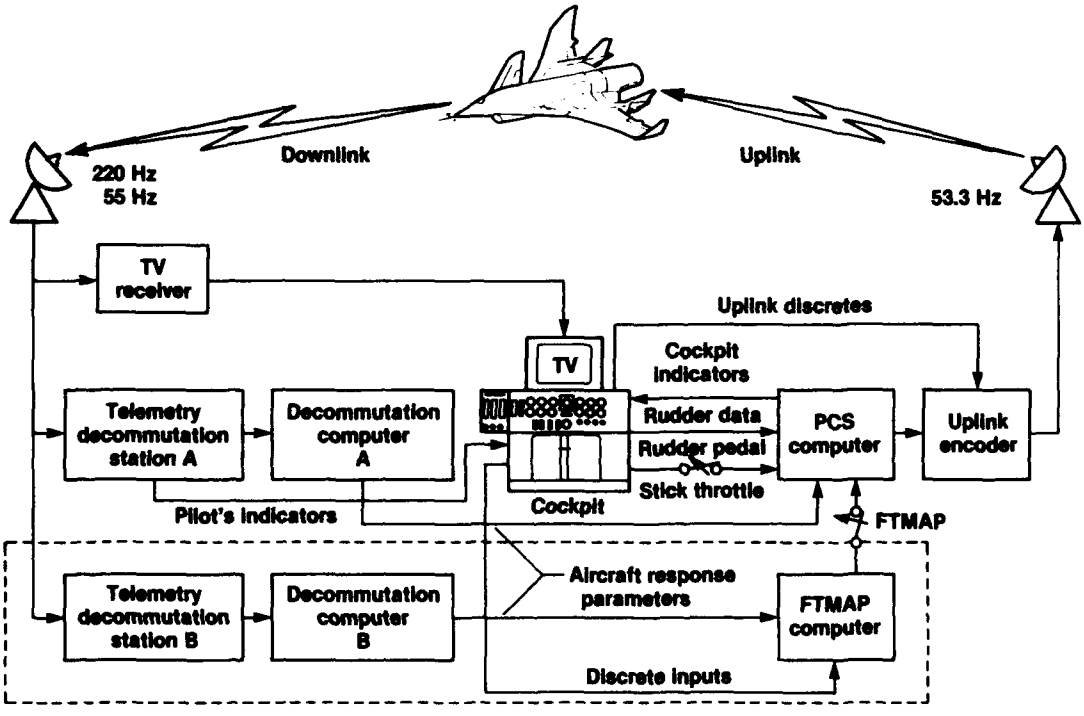

Figure 26. HiMAT flight system with FTMAP.

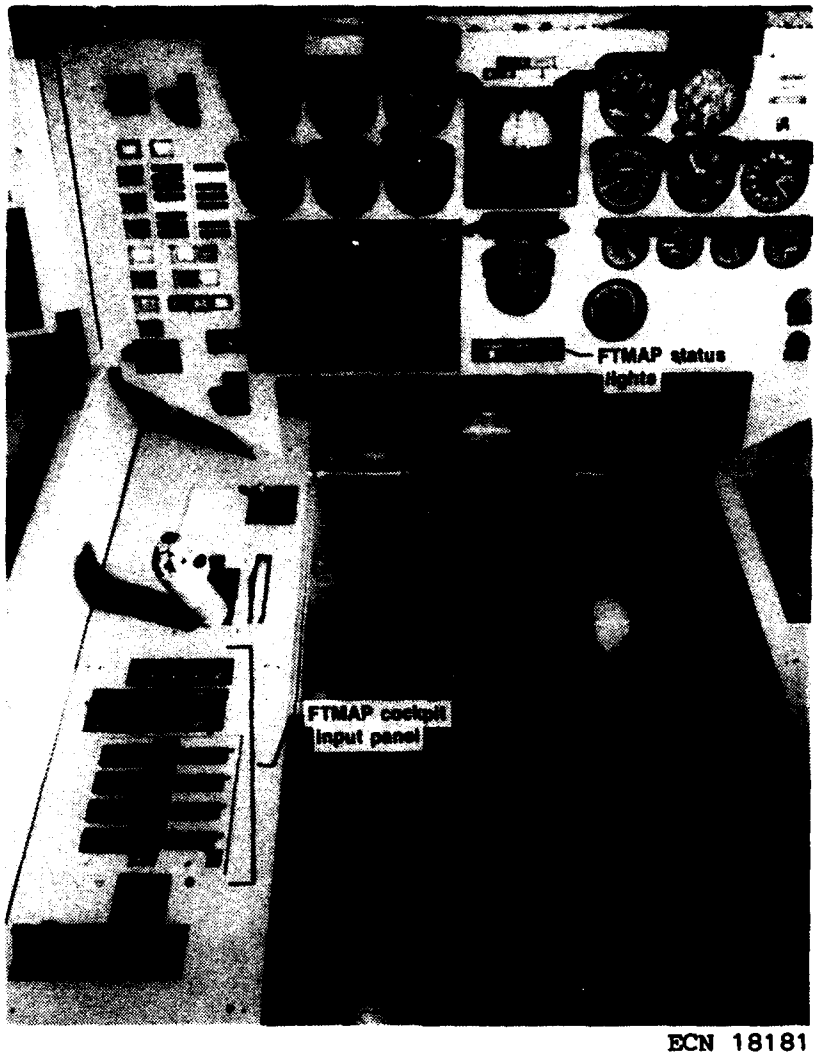

ECN 18181

Figure 27. HiMAT cockpit showing FTMAP hardware.

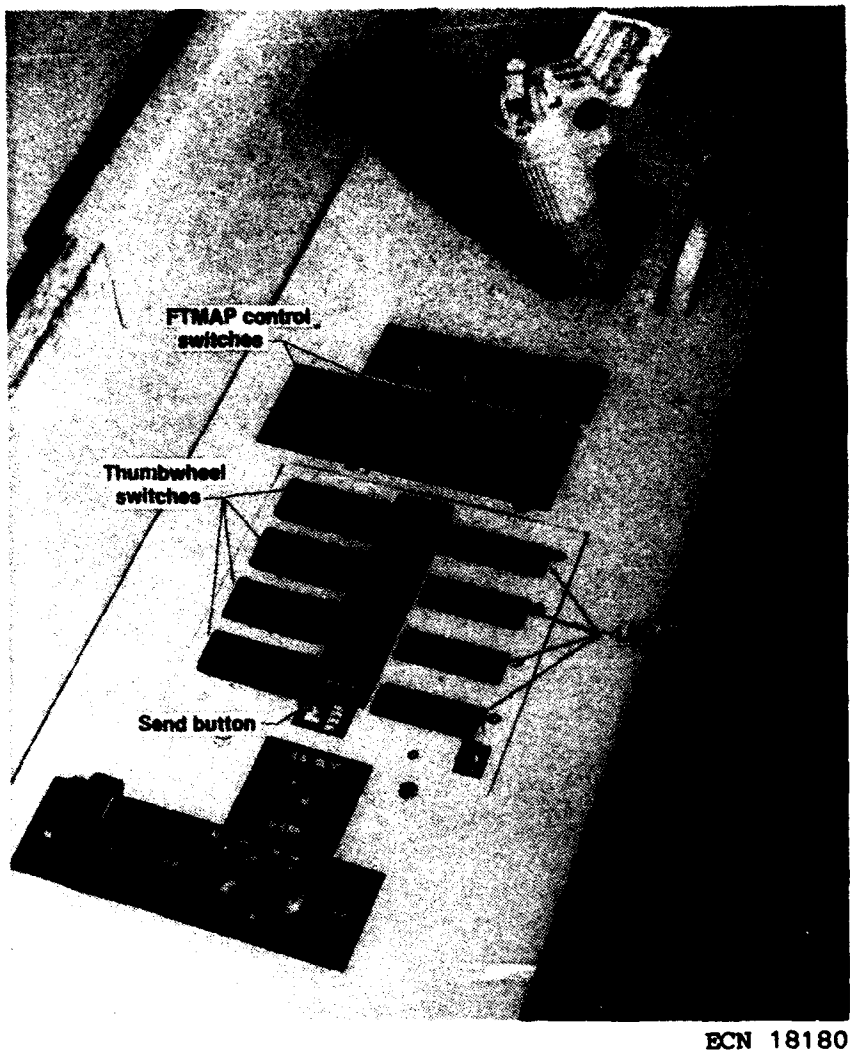

Figure 28. FTMAP cockpit input panel.

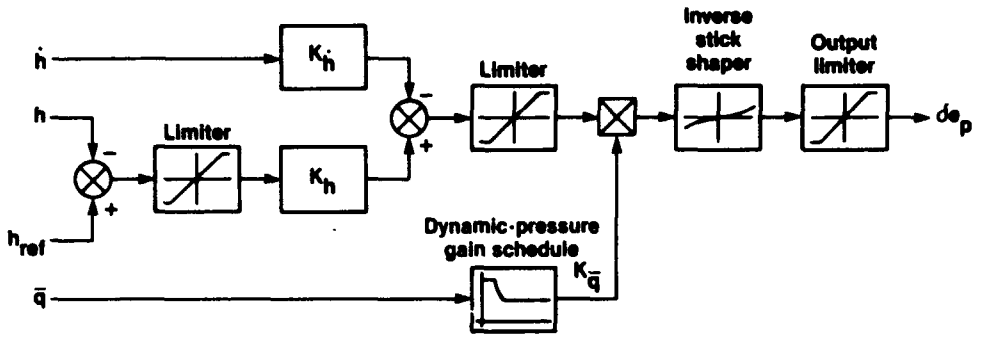

Figure 29. Altitude-hold mode.

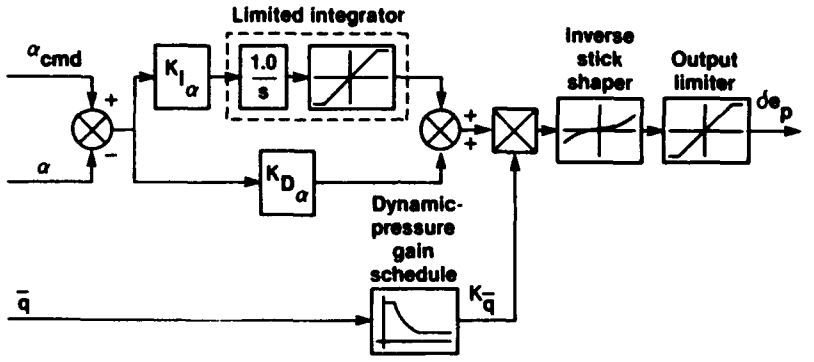

Figure 30. Angle-of-attack control mode.

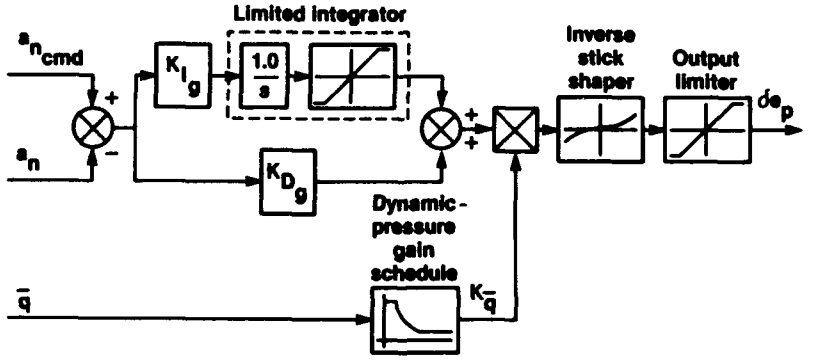

Figure 31. Normal-acceleration control mode.

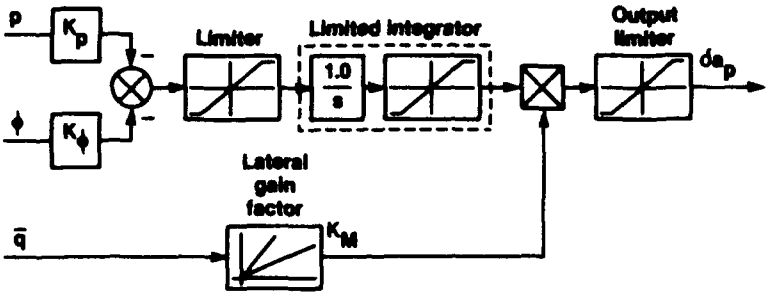

Figure 32. Wings-level control mode.

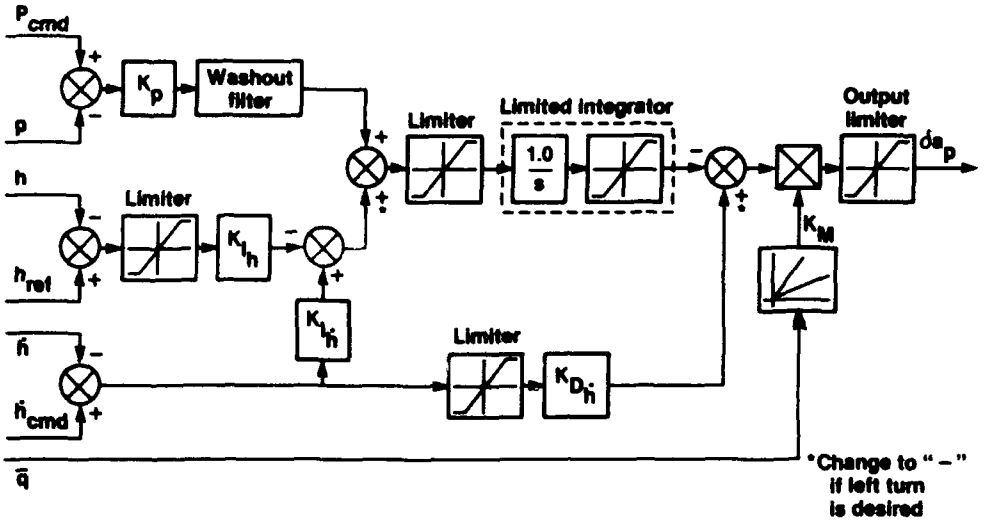

Figure 33. Turn control mode.

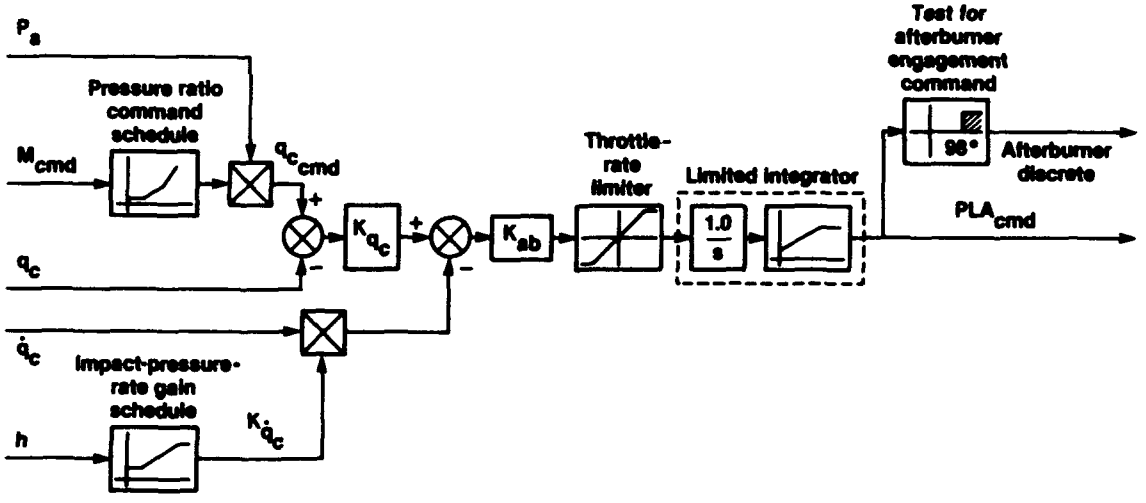

Figure 34. Throttle control mode.

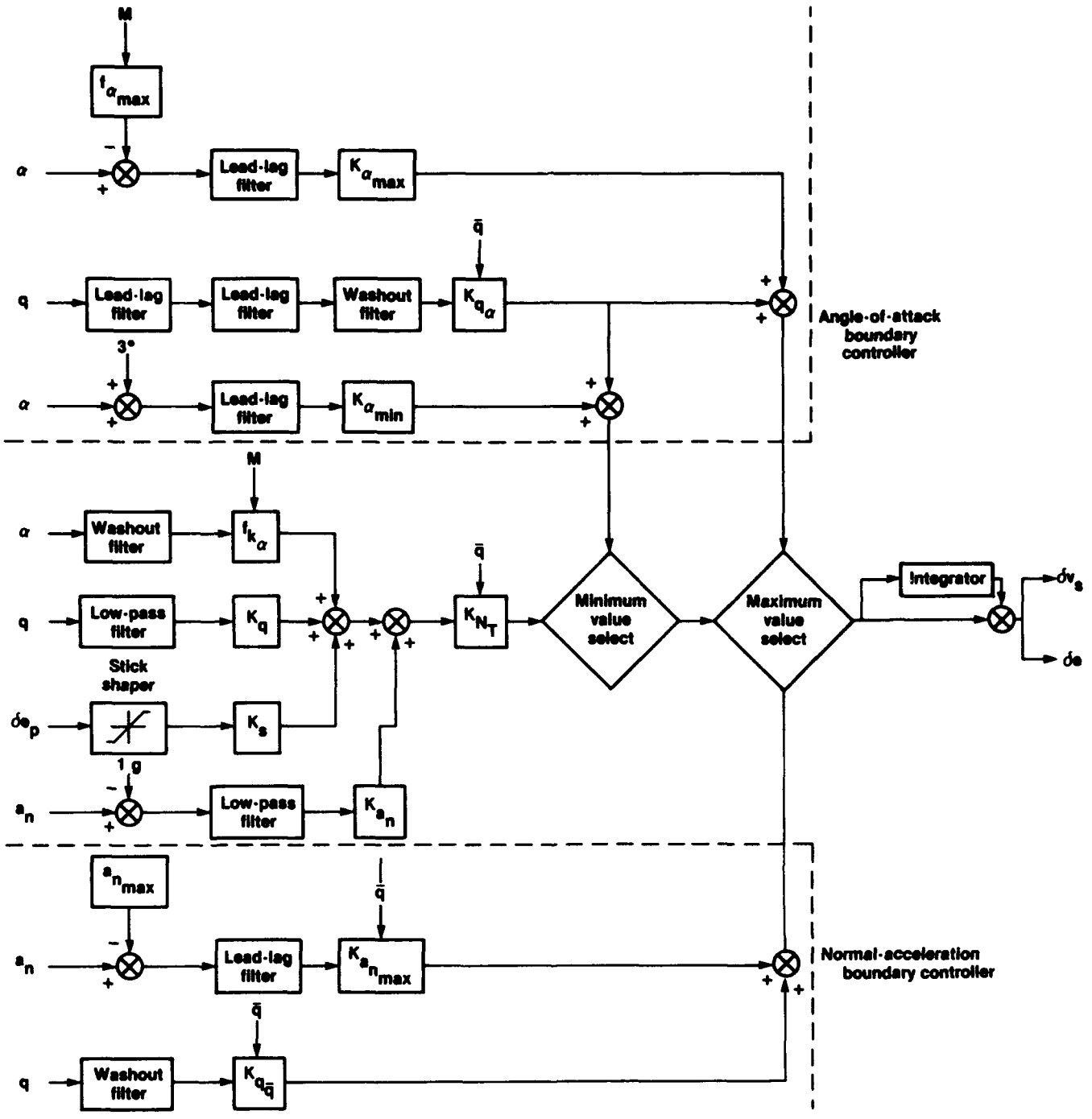

Figure 35. Pitch axis of HiMAT primary control system.

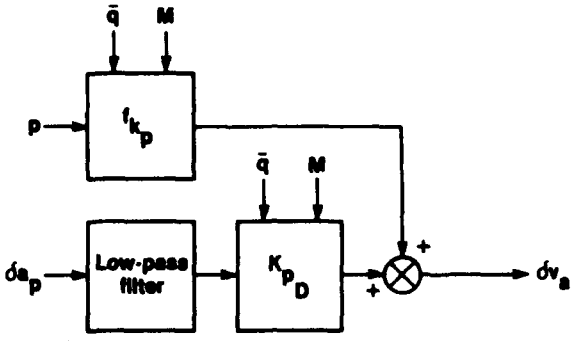

Figure 36. Roll axis of HiMAT primary control system.

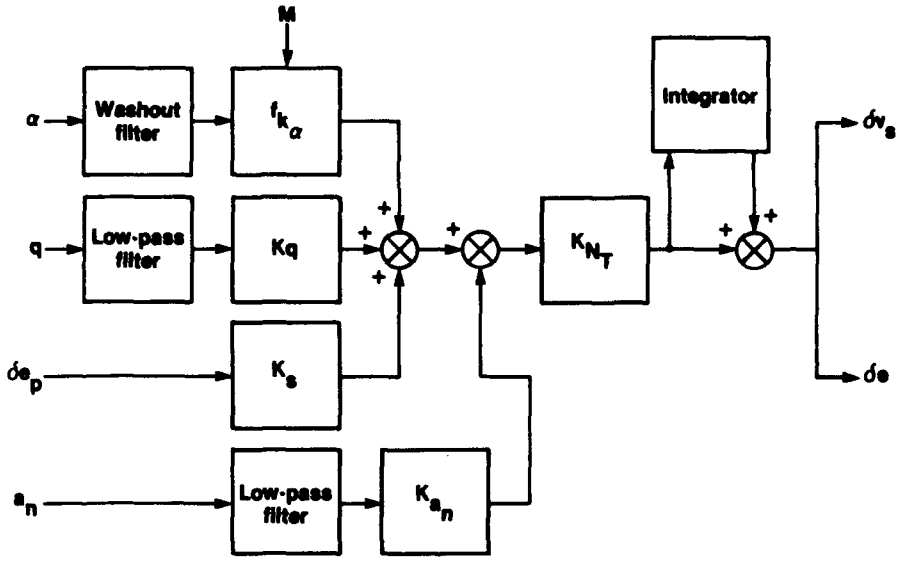

Figure 37. Linear model of pitch axis of HiMAT primary control system.

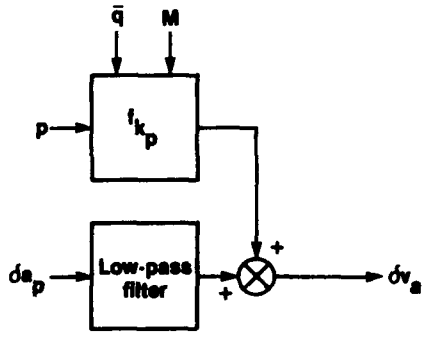

Figure 38. Linear model of roll axis of HiMAT primary control system.

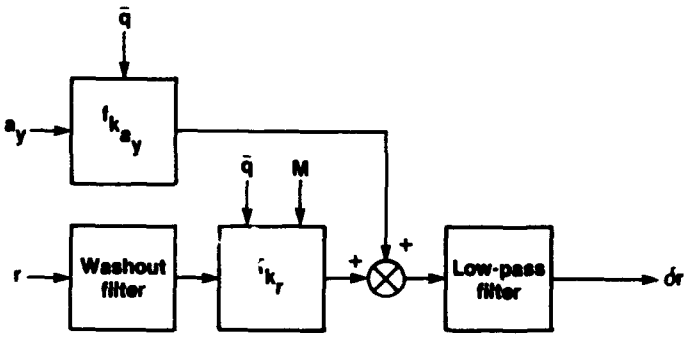

Figure 39. Linear model of yaw-axis feedback of HiMAT primary control system.

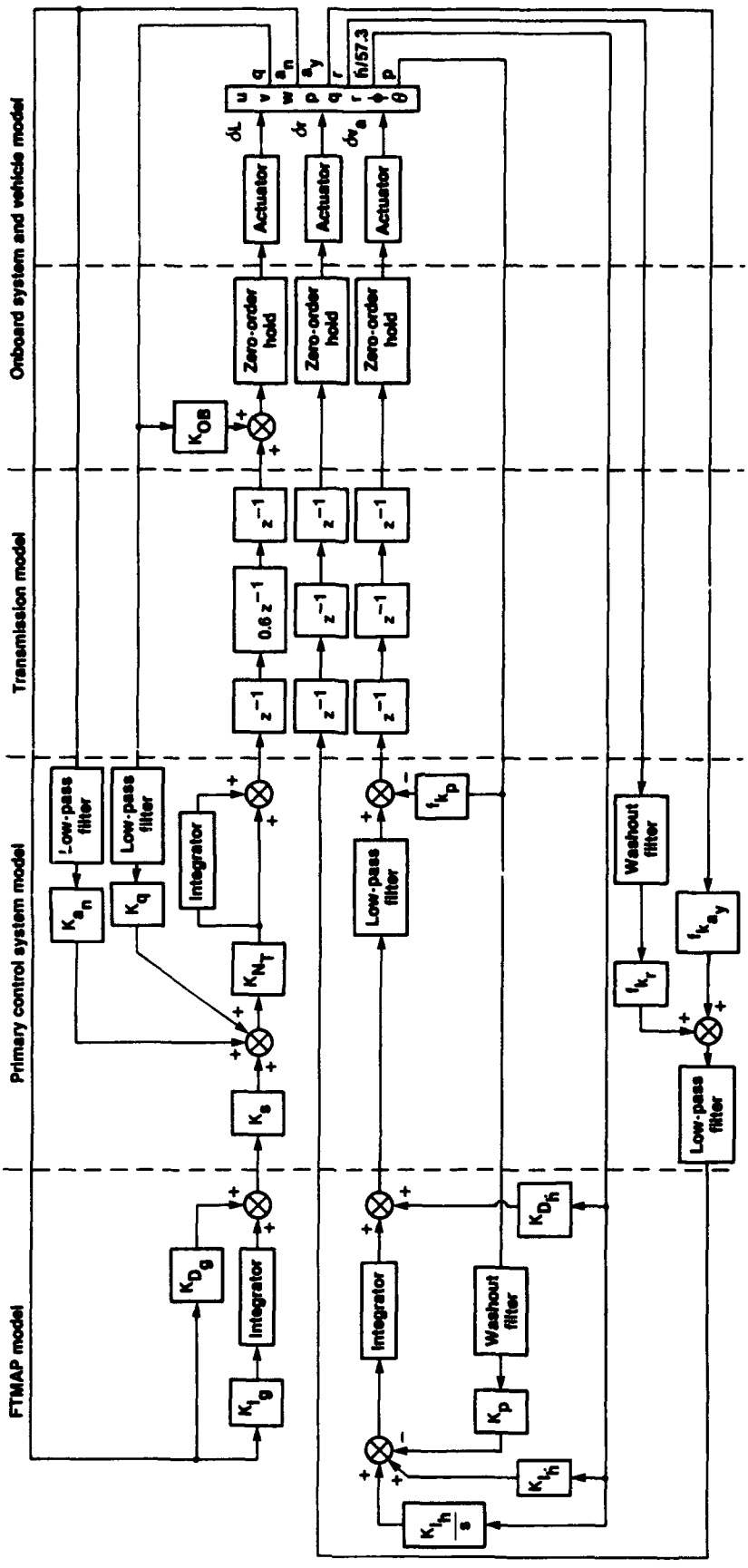

Figure 40. Linear model for normal-acceleration commanded turn.

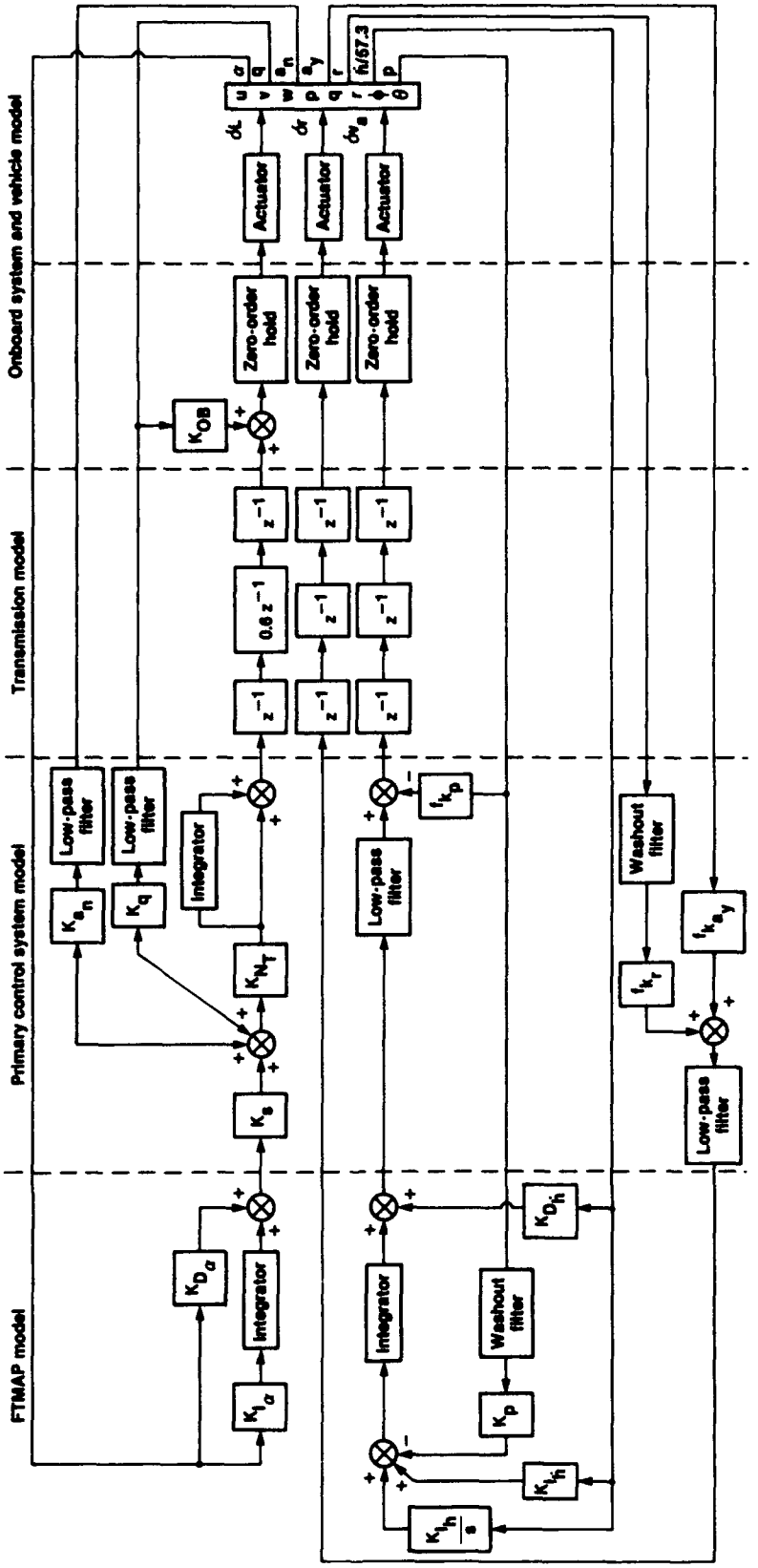

Figure 41. Linear model for angle-of-attack commanded turn.

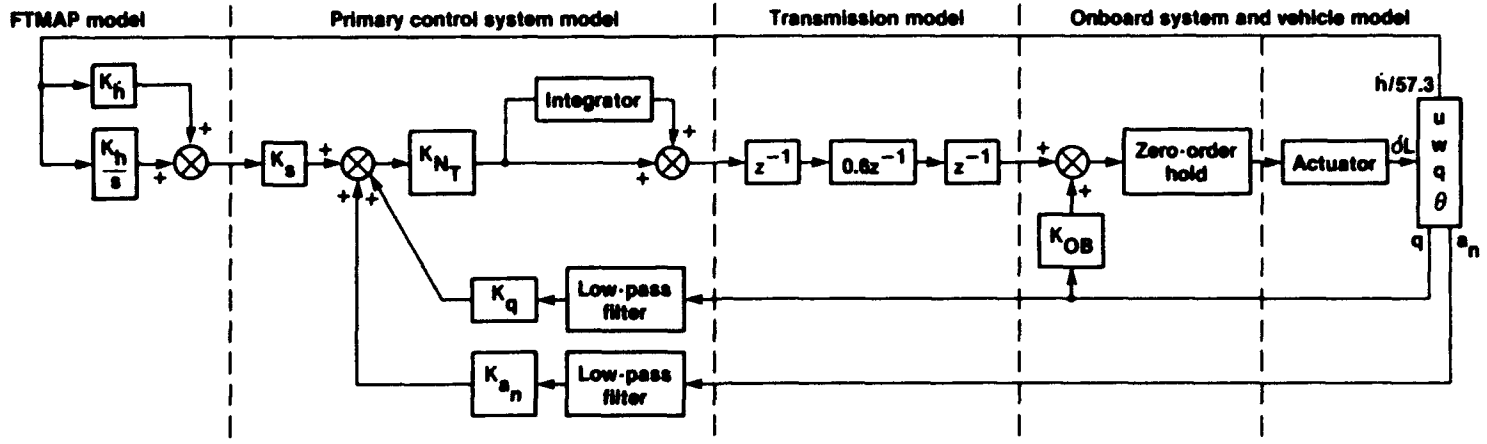

Figure 42. Altitude-hold model.

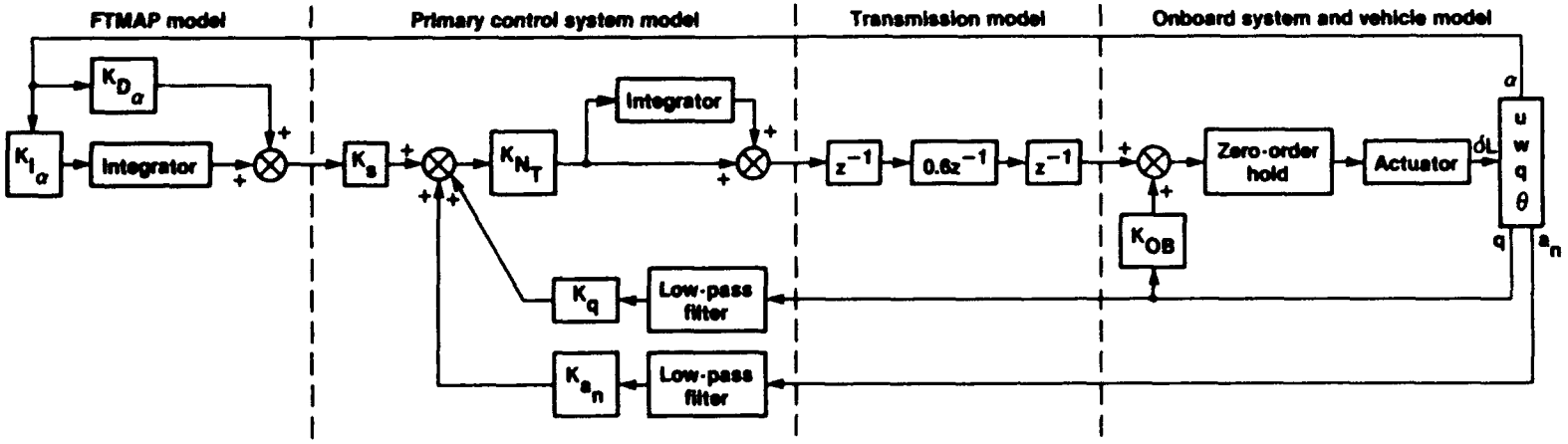

Figure 43. Pushover-pullup linear model.

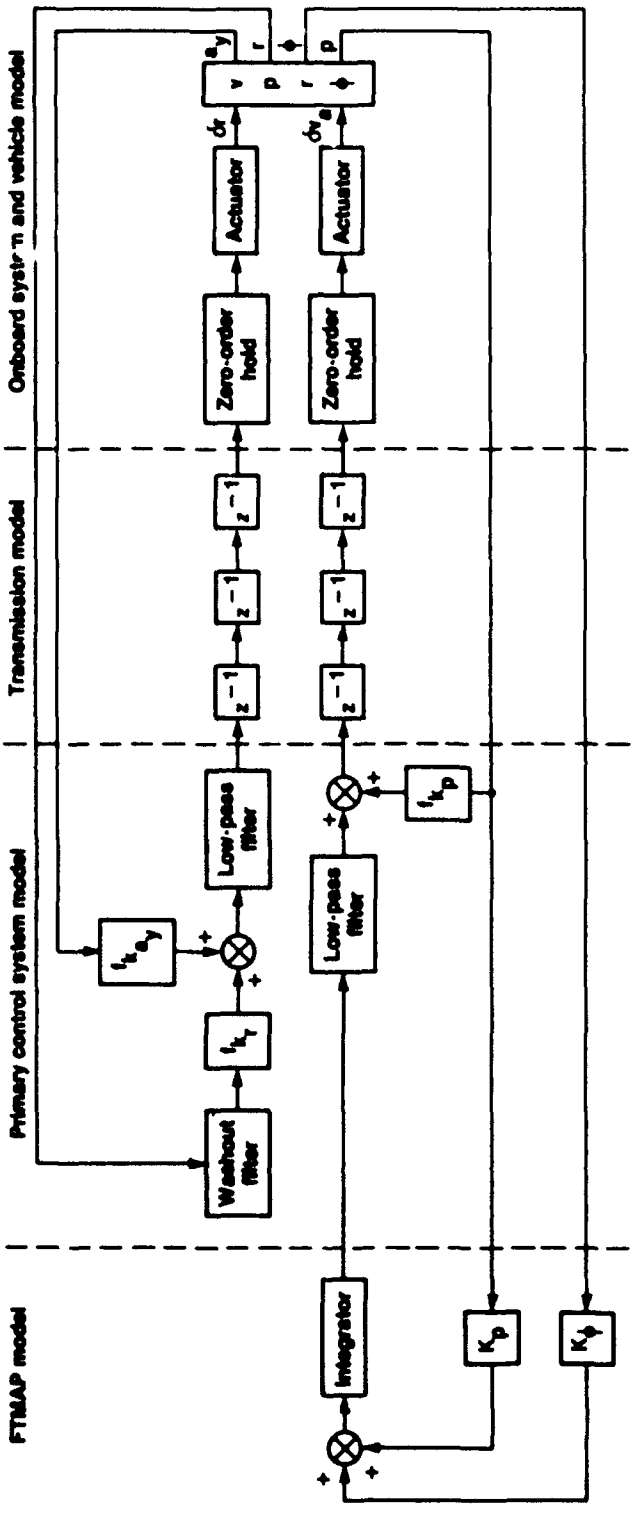

Figure 44. Wings-level linear model.

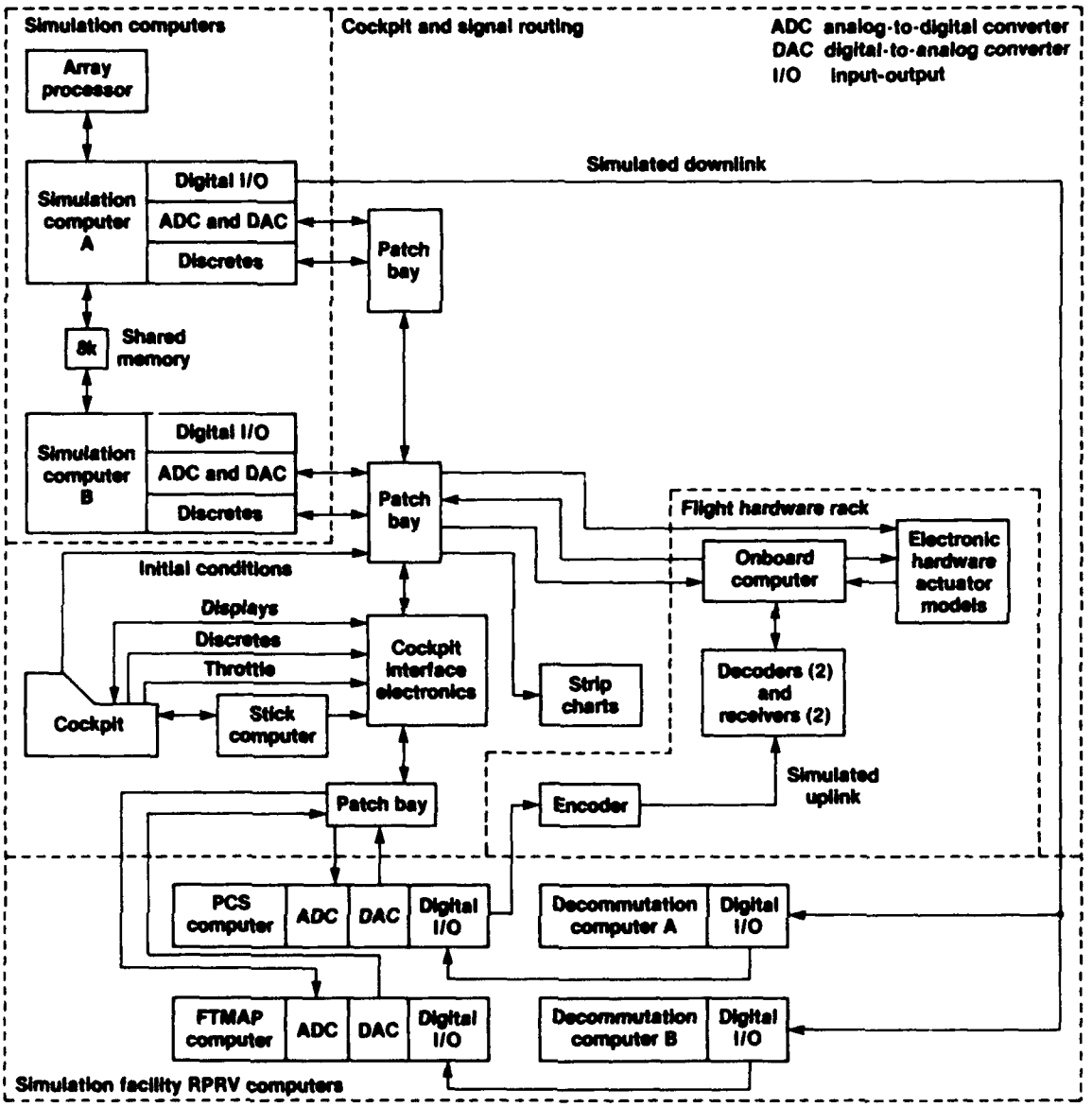

Figure 45. HiMAT-FTMAP simulation system.

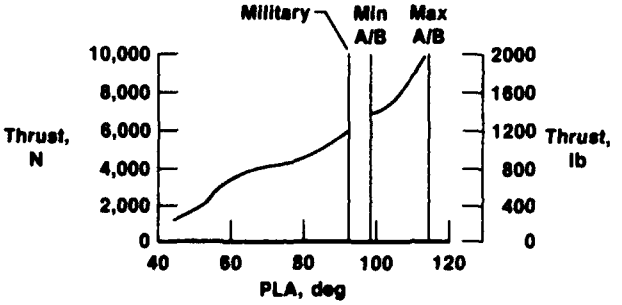

Figure 46. Predicted thrust as a function of power lever angle for HiMAT J85-21 engine.

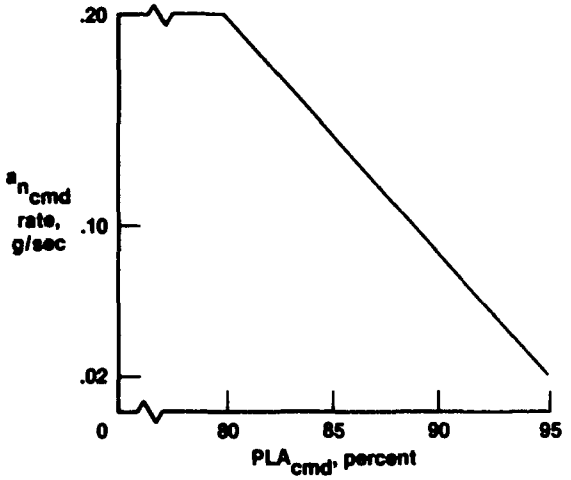

Figure 47. Normal-acceleration command rate for rocking-horse maneuver.

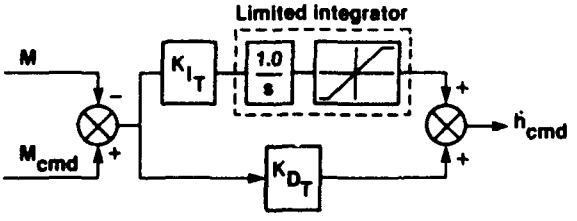

Figure 48. Altitude-rate command for thrust-limited windup turn.

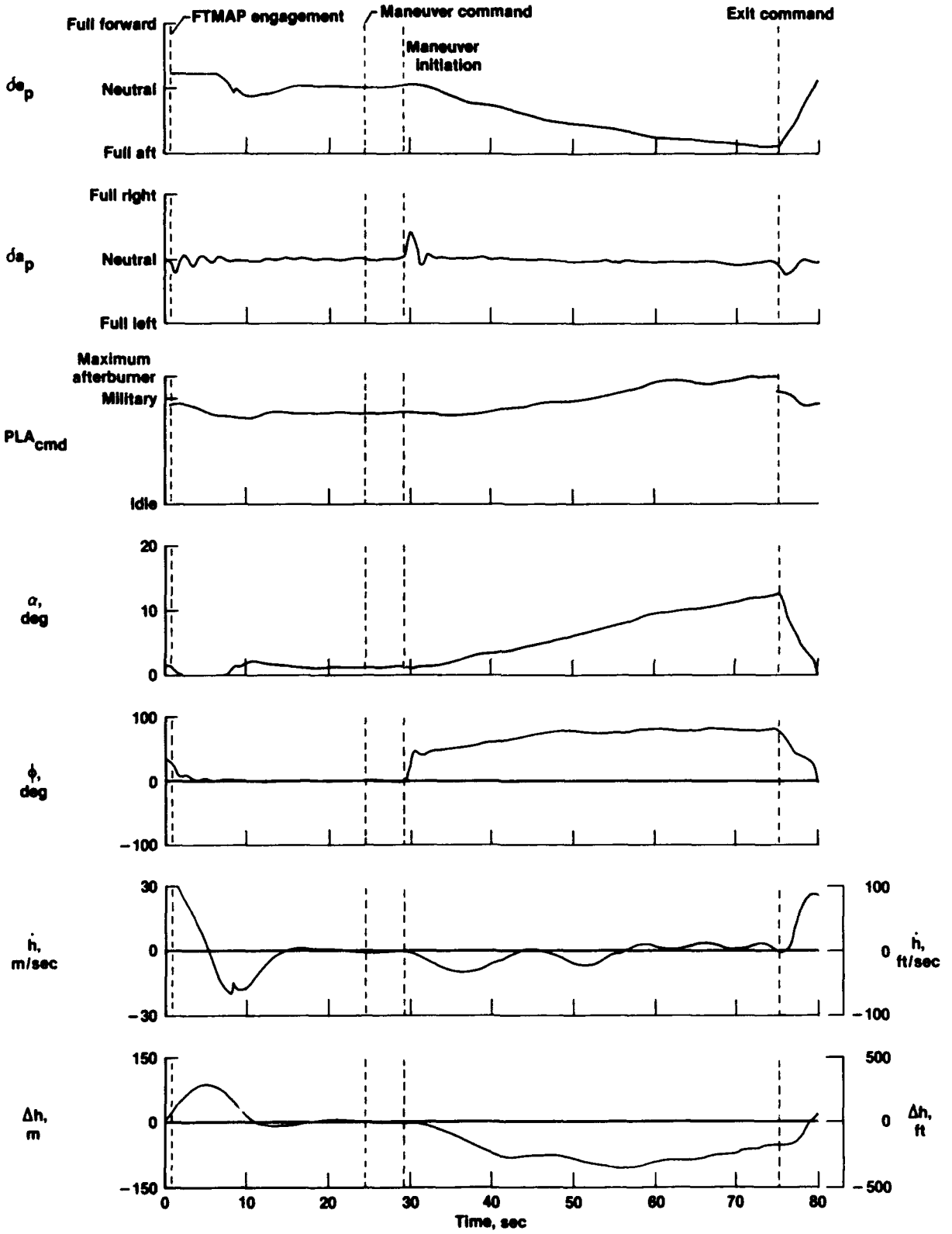

Figure 49. Windup turn using simulation at Mach 0.90 and 7600-m (25,000-ft) altitude.

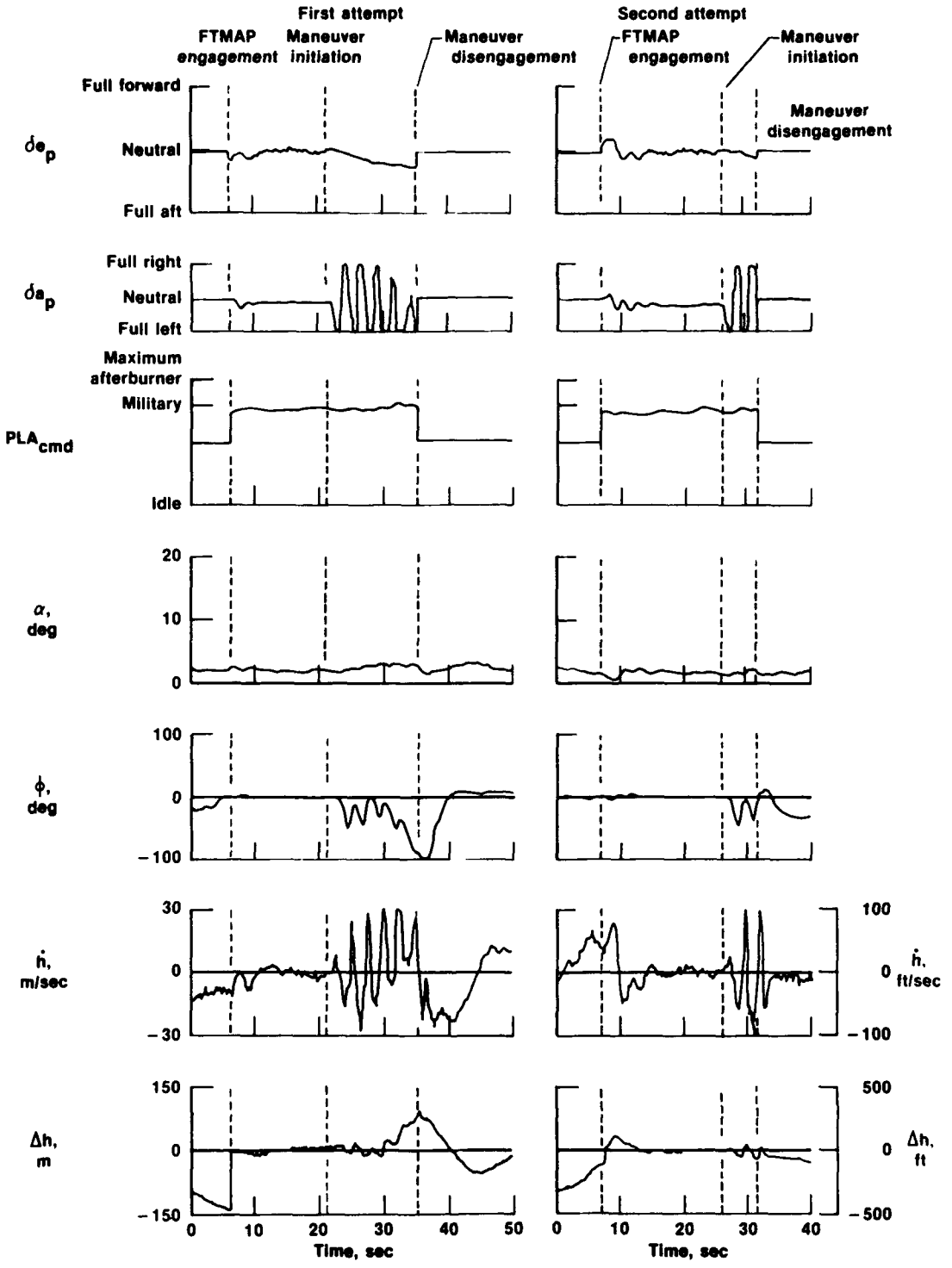

Figure 50. Comparison of first and second flight attempts of windup turn at nominal conditions of Mach 0.90 and 7600-m (25,000-ft) altitude.

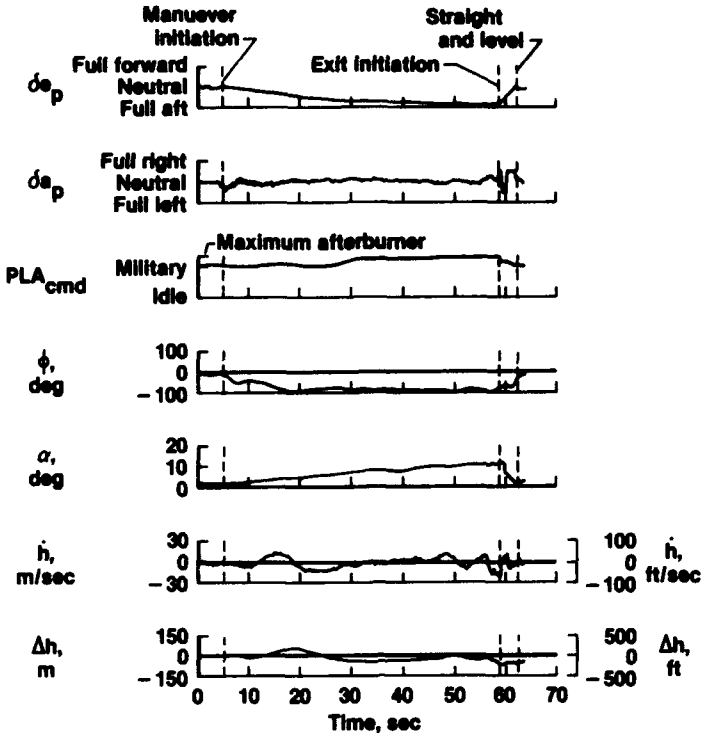

Figure 51. Windup turn with modified bank-angle command initiation at nominal conditions of Mach 0.90 and a 7600-m (25,000-ft) altitude.

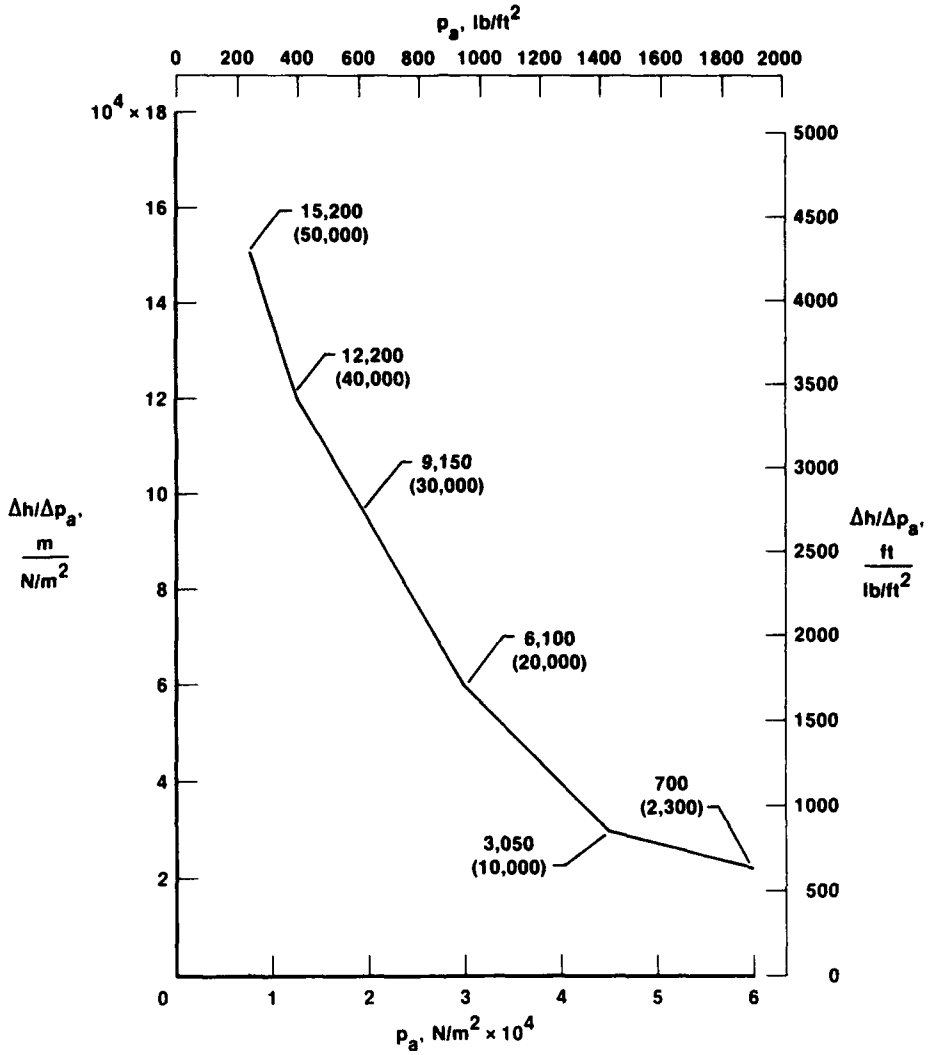

Figure 52. Ratio of altitude to static pressure. (Altitude points are indicated in meters (feet).)

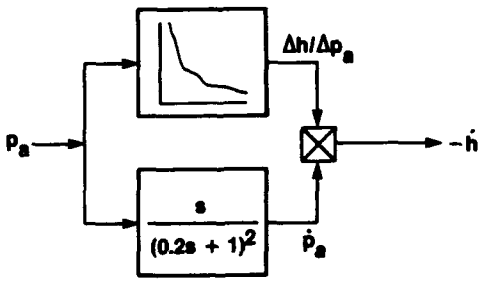

Figure 53. Block diagram of HiMAT altitude-rate computation.

1. Report No.	2. Government Accession No.	3. Recipient's Catalog No.
NASA TP-2618		

4. Title and Subtitle	5. Report Date
Development and Flight Test of an Experimental Maneuver Autopilot for a Highly Maneuverable Aircraft	September 1986
	6. Performing Organization Code

7. Author(s)	8. Performing Organization Report No.
Eugene L. Duke, Frank P. Jones, and Ralph B. Roncoli	H-1258
	10. Work Unit No. RTOP 533-02-71

9. Performing Organization Name and Address	11. Contract or Grant No.
NASA Ames Research Center Dryden Flight Research Facility P.O. Box 273 Edwards, CA 93523-5000	

12. Sponsoring Agency Name and Address	13. Type of Report and Period Covered
National Aeronautics and Space Administration Washington, D.C. 20546	Technical Paper
	14. Sponsoring Agency Code

15. Supplementary Notes

16. Abstract

This report presents the development of an experimental flight test maneuver autopilot (FTMAP) for a highly maneuverable aircraft. The essence of this technique is the application of an autopilot to provide precise control during required flight test maneuvers. This newly developed flight test technique is being applied at the Dryden Flight Research Facility of NASA Ames Research Center. The FTMAP is designed to increase the quantity and quality of data obtained in flight test. The technique was developed and demonstrated on the highly maneuverable aircraft technology (HiMAT) vehicle. This report describes the HiMAT vehicle systems, maneuver requirements, FTMAP development process, and flight results.

17. Key Words (Suggested by Author(s))	18. Distribution Statement
Aircraft guidance, Aircraft control, Flight test techniques, Flight test maneuver autopilot (FTMAP), Highly maneuverable aircraft technology (HiMAT)	Unclassified — Unlimited STAR category 05

19. Security Classif. (of this report)	20. Security Classif. (of this page)	21. No. of Pages	22. Price*
Unclassified	Unclassified	59	A04

*For sale by the National Technical Information Service, Springfield, Virginia 22161.

NASA-Langley, 1986